

WHOI-74-89

Copy 2

Woods Hole
Oceanographic
Institution



W.H.O.I./BROWN CTD MICROPROFILER:
METHODS OF CALIBRATION AND DATA HANDLING

By

N. P. Fofonoff, S. P. Hayes, and
R. C. Millard, Jr.

December 1974

TECHNICAL REPORT

*Prepared for the Office of Naval Research
under Contract N00014-74-CO262; NR 083-004.*

*Approved for public release; distribution
unlimited.*

WHOI-74-89

W.H.O.I./BROWN CTD MICROPROFILER: METHODS OF
CALIBRATION AND DATA HANDLING

By

N. P. Fofonoff, S. P. Hayes, and R. C. Millard, Jr.

WOODS HOLE OCEANOGRAPHIC INSTITUTION
Woods Hole, Massachusetts 02543

December 1974

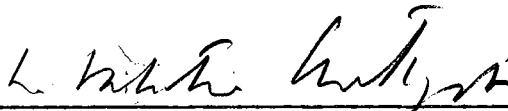
TECHNICAL REPORT

*Prepared for the Office of Naval Research
under Contract N00014-74-CO262; NR 083-004.*

*Reproduction in whole or in part is permitted
for any purpose of the United States Government.
In citing this report in a bibliography, the
reference should be followed by the phrase:
UNPUBLISHED MANUSCRIPT.*

*Approved for public release; distribution
unlimited.*

Approved for Distribution



L. Valentine Worthington, Chairman
Department of Physical Oceanography

Table of Contents

	<u>Page No.</u>
ABSTRACT	i
ACKNOWLEDGEMENTS	ii
INTRODUCTION	1
I. CALIBRATIONS IN THE LABORATORY AND FIELD TEMPERATURE	3
A. Temperature	3
B. Pressure	5
C. Conductivity	7
D. Down-Up Comparisons	14
II. TEMPERATURE LAG CORRECTIONS	16
A. Lag Correction Scheme	16
B. Effect of Instrument Noise	18
C. Frequency Response	20
D. Selecting the Temperature Probe Time Constant	25
E. A Uniform Pressure Series and Error Estimates	28
III. THE SALINITY ALGORITHM	30
A. Temperature Conversion	30
B. Conductivity Ratios	31
C. Computational Procedure	33
SUMMARY	34
APPENDIX I: Empirical Formulas	35
APPENDIX II: Conductivity Calibration Technique	39
REFERENCES	42
FIGURE CAPTIONS	44
TABLE CAPTIONS	46

ABSTRACT

This report describes calibration techniques developed over the past three years for the WHOI/Brown CTD in the Moored Array Program. Comparison is made with classical methods of hydrography for stations obtained in the MODE-1 density program. Methods for temperature lag correction and conversion of conductivity to salinity are given.

ACKNOWLEDGEMENTS

The authors wish to thank Doris Haight and Betty Stuermer for preparing the text and figures; Al Bradshaw and Karl Schleicher for comments on the text, and Doug Moore, Mike Parke, and Gordon Volkmann for help in collecting and processing the data. This work was supported by ONR Contract N00014-74-CO262; NR 083-004 and NOAA Contract 03-4-022-31.

INTRODUCTION

In January, 1972 the Moored Array Project at W.H.O.I. began routine use of the newly developed W.H.O.I./Brown CTD for vertical profiling of temperature and salinity. The instrument used was a prototype of the final W.H.O.I./Brown CTD (see Brown, 1974 for a discussion of the technical details of the final CTD). The prototype instrument has a miniature (8 mm long, 2 mm I.D.) four-electrode conductivity cell. The temperature is sensed with a platinum resistance thermometer and pressure with a strain gauge bridge transducer. The temperature sensor is the main difference between the final (Brown, 1974) and the prototype CTD with fast response thermistor being added for the final version.

The W.H.O.I./Brown CTD is a ship-lowered instrument. It digitizes conductivity, temperature, and pressure in the lowered unit. This information is telemetered to the deck unit along single conductor-shielded cable. The resolution is .001 mmho/cm in conductivity, .0005 °C in temperature, and .1 decibar in pressure. The data are recorded in digital form on a 9-track type using a Hewlett-Packard 2116 computer. Subsequent processing (e.g., editing, salinity calculating, and pressure smoothing) is done on this recorded series.

The instrument sampling rate is 30 Hz. The prototype unit has a temperature response time of roughly 200 msec compared to a conductivity cell flushing time of roughly 30 msec. In order to

calculate accurate salinities, this response time discrepancy must be compensated.

The operational experience detailed in this report was accumulated during 1972 and 1973 largely in the MODE-O and MODE-I field experiments. Over 200 stations have been considered. In order to obtain precision results the CTD was calibrated in the laboratory and the calibration was monitored by collecting water samples at sea. The details of the calibration techniques are discussed in the following section. The results demonstrate that the CTD is capable of producing temperature, salinity, and pressure measurements with a precision equal to or exceeding those obtained with standard hydrographic techniques.

I. CALIBRATIONS IN THE LABORATORY AND FIELD TEMPERATURE

A. Temperature

Laboratory Temperature Calibration

The CTD temperature sensor has been calibrated directly and indirectly against a Leeds and Northrop platinum wire temperature probe and Guildline bridge. The L&N platinum thermometer was first standardized against a triple point cell. The platinum thermometer is calibrated on the 1968 International Practical Temperature Scale (IPTS).

Normally the CTD was not compared directly to the delicate platinum thermometer. Rather the platinum thermometer calibration was transferred to a Hewlett-Packard Quartz thermometer; and the CTD was then compared to the Quartz thermometer. The advantages of the Quartz thermometer are that it is less delicate, more portable, and displayed in engineering units. Two techniques were used for temperature calibration. The entire instrument was immersed in a large circulating salt water bath or just the conductivity and temperature sensors were placed in a covered, stirred vacuum flask. The bath has the advantage of cooling the CTD temperature circuits thus calibrating out any temperature drift in the electronics. The two techniques yielded identical results within the experimental accuracy for the one instrument considered.

There are four principal sources of temperature calibration uncertainty. 1) Temperature gradients in the bath can be up to 2 millidegrees. 2) Heat transfer along the thermometer stem

can be made small by sufficient immersion length (N.B.S. Monograph 126, 1973). 3) Uncertainty of digital readout of CTD deck unit and Quartz thermometer is one millidegree. 4) Linearity of CTD temperature circuit $\pm .0015$ °C (Brown, 1974).

Six calibrations of the CTD over a 16-month period show the CTD temperature calibration to have shifted 5 millidegrees (see Figure 1). The shift in temperature offset occurred between October and December 1973 as opposed to a gradual drift.

In situ Temperature Check

During MODE-I a large number of comparisons were made between the CTD and deep-sea reversing thermometers (DSRT) calibrated by Geof Whitney at W.H.O.I. A total of 175 of a possible 198 comparisons below 4.5 °C are shown in the histogram of temperature differences between DSRT and the CTD (Figure 2). Most of the DSRT were -2 to 6 °C range. These thermometers have .02 °C graduations and readings were reported to .005 °C or better. Temperature differences exceeding $\pm .04$ °C were rejected as spurious. A detailed discussion of DSRT accuracies is given by (Boyce, 1966). The mean error between the CTD and DSRT is $-.5$ m °C and the standard deviation is 10 m °C. Part of the reason for the large standard deviations of temperature differences are systematic differences between reversing thermometers. For example, the secondary peak at $+8$ m °C is due to thermometer #3048. The most probable temperature difference is $+.002$ to $.003$ °C which is roughly the difference between the 1948

and 1968 IPTS at a temperature of 3 °C. The DSRT were calibrated to the 1948 IPTS while the CTD used the 1968 IPTS.

B. Pressure

Laboratory Pressure Calibration

The laboratory calibration of pressure uses a piston gauge standard made by the American Instrument Company. The manufacturer quotes absolute errors of .05 percent for pressure data. The types and magnitudes of the errors (Cross, 1963) are as follows: 1) Local gravity adjustment of weights from a standard gravity of $g = 980.665 \text{ cm/sec}^2$; Woods Hole, MA $g = 980.323 \text{ cm/sec}^2$ or a .04% decrease in pressure. 2) Air buoyancy correction to weights equals a .014% decrease in pressure. 3) Fluid head offset of pressure of + .7 decibars. 4) Thermal expansion of the piston is .0016% per degree centigrade away from 20 °C. 5) Elastic distortion pressure error of the piston (Johnson and Newhall, 1953) which for the AMINCO piston gauge is

$$P_T = P_O / (1 + 3.55 \cdot 10^{-8} P_O);$$

$$P_T = \text{pressure decibars}; \quad (1)$$

$$P_O = \text{observed pressure.}$$

At 5000 decibars elastic piston distortion yields an error of .02%. Notice that most corrections are in the same direction and make the apparent piston gauge pressure too high.

The corrections listed were applied to the raw piston gauge pressure data. A CTD correction graph (corrected piston gauge pressure-nominal CTD pressure) is plotted versus pressure in Figure 3. It shows a non-linear behavior of the CTD amounting to 4.5 decibars at mid-range. A quadratic correction was applied to the CTD pressure between 0-4000 decibars and a constant offset above 4000 decibars (see Figure 3) to bring the CTD to within 1.5 decibars of the piston gauge at all pressures.

In situ Pressure Check

During the MODE density program the CTD pressure was compared to thermometric pressure readings using unprotected thermometers calibrated by Geof Whitney. Details of the calibration procedure used by Whitney are given in (Whitney, 1957). The temperature used to compute the thermometric pressure was obtained from the corrected CTD temperature. The deep unprotected thermometers are graduated at .2 °C intervals. Whitney estimates the uncertainty of individual thermometer readings (Whitney, 1957) corresponds to an R.M.S. thermometric pressure error of 4.5 decibars. The thermometric pressure was computed by the formula:

$$P = \frac{g(T_u - T_{CTD}) 10}{1000 Q} \text{ (decibars)}$$

$$g = 983.323 \text{ cm/sec}^2 \text{ at Woods Hole, MA}$$

$$T_u = \text{unprotected thermometer temperature} \quad (2)$$

$$T_{CTD} = \text{CTD temperature}$$

Q is the scaling factor between temperature readings of individual unprotected thermometers and pressure in kilograms/cm².

A (thermometric-CTD (uncorrected)) pressure correction curve is given in Figure 3. Each pressure difference is an average of a number of observations as indicated on the graph. Pressure differences exceeding 10 decibars were not included in (thermometric-CTD) pressure comparisons. The (thermometric-CTD) pressure correction curve is noisier than that obtained from the piston gauge but it does not show any systematic difference from the piston gauge to indicate temperature sensitivity of this particular CTD strain gauge pressure transducer. Down versus up CTD comparisons discussed later further confirms this observation.

A histogram of 189 (thermometric-CTD (uncorrected)) pressure differences for all pressure levels is given in Figure 4. The distribution of differences is consistent with the RMS error of 4.5 decibars obtained from Whitney's data (Whitney, 1957). The average pressure difference was found to be -1.7 decibars which is reduced when the piston gauge pressure correction is applied to the CTD and the .5 decibar vertical separation between thermometric and CTD pressure sensors is subtracted from the CTD.

C. Conductivity

The conductivity, temperature, and pressure must be measured simultaneously to compute salinity. The conductivity is

calibrated through salinity, thus temperature and pressure sensors must be well calibrated.

Laboratory Calibration

The conductivity calibration is obtained by immersing the conductivity and temperature sensors in a covered vacuum flask filled with stirred Copenhagen Standard sea water. Standard water with a known salinity is used to determine the adjustment necessary to the CTD conductivity in order that the computed CTD salinity matches the Standard Water salinity. The CTD temperature sensor must be calibrated before calibrating conductivity.

The CTD makes a measurement proportional to the conductance -G- of a volume of sea water inside and in the immediate vicinity of the conductivity cell. Conductance (G) is related to conductivity (γ) by the geometry of the conductivity cell. Notice the equation relating the two says that reducing the cross-sectional area (R^2) (as coating the interior of the cell will do) reduces the measured conductance and therefore the inferred conductivity.

$$G = \gamma \frac{R^2 \pi}{\ell} \quad \text{where} \quad \frac{\ell}{\pi R^2} \quad \text{is the cell factor} \quad . \quad (3)$$

The size of the conductivity cell also varies with temperature and pressure. These corrections are discussed under vertical variations.

The conductivity cell requires continual recalibration at sea because of drift in conductivity between stations. Conductivity

shifts of as much as .013 mmho/cm (\sim .015 ppt) occurred between stations during MODE. To compensate for the changing conductivity, a cell factor is computed for each station. The cell factor is the scaling factor the measured conductivity must be multiplied by to obtain the "true" conductivity. The variation of the cell factor is probably due to small changes in cell dimensions caused by deposition and washing off of material from the inner cell surface. The in situ conductivity calibration is obtained through salinity by a technique discussed in Appendix II.

Sources of Error in Conductivity

A coating of 3×10^{-5} mm on the inside of the 2 mm I.D. conductivity cell will reduce the measured conductivity .001 mmho/cm. Pressure and temperature change the dimensions of the alumina conductivity cell: A pressure change of 1500 decibars yields a .001 mmho/cm shift and a temperature change of 3 °C yields the same change, to the measured conductivity. Because the conductivity calibration is obtained from salinity, an error of 1 milli-degree in the temperature or an error of 2.5 decibars in pressure introduces roughly a .001 mmho/cm conductivity error.

In situ Calibration

Because conductivity is so sensitive to a coating of material inside the cell, frequent recalibration at sea is required to obtain reliable salinities. To obtain calibration salinities, water samples are collected during a station using a Rosette

sampler mounted .5 meters above the CTD sensors. A thermostatic salinometer is used to obtain salinities from the water samples at sea. Individual calibration salinities have an uncertainty of $\pm .003$ ppt (see Figure 7). Averaging of the water sample salinities is necessary to reduce the uncertainty in the conductivity calibration. The method of averaging adopted for MODE involved constructing an average potential temperature-salinity diagram for the North Atlantic Deep Water. The water bottle salinities compared well with historic θ/s curves of Worthington-Metcalf and Crease in the range of θ from 2.55 to 2.05 $^{\circ}\text{C}$, as shown in Figure 5. Crease's θ/s was adopted as the salinity standard for the MODE data. The calibration technique involved computing an average conductivity cell factor from θ/s salinities obtained every .05 $^{\circ}\text{C}$ potential temperature over the range 2.55 to 2.05 $^{\circ}\text{C}$. This technique requires deep stations to 4000 meters. For shallower stations, calibration was made against individual station water sample salinities.

Conductivity Drift

The CTD conductivity changed over the MODE experiment by as much as .013 mmho/cm ($\sim .015$ ppt) between stations. A graph of the cell factor (C.F.) time variations is shown in Figure 6. A larger C.F. implies a smaller measured conductivity which is consistent with cell coating. The graph suggests that a coating process occurs on deck between stations. Frequent stations show a reduction

of the C.F. (self-cleaning) while long periods on deck result in a shift towards a higher C.F. Rinsing of the conductivity cell in .1 normal HCL acid cleans the cell (i.e., shifts towards lower C.F.). The noisy C.F. values in Figure 6 for June are due to calibrating to individual station water sample salinities because stations were not taken deep enough (1700 decibars) to use the North Atlantic deep water θ/S .

Summary of Salinity Comparison Result

Two hundred and sixty-nine of the CTD-Rosette salinities comparisons collected during the MODE density program are summarized in a histogram of salinity differences in Figure 7. The Rosette salinities were collected throughout most of the water column at the same time as the CTD measured salinity but the Niskin bottles were .5 meters shallower than the CTD sensors. The average salinity difference is .0002 0/00. The standard deviation of salinity differences is (.0024 0/00) which is about the same scatter obtained from duplicate salinity samples run on the thermostatic salinometer .003 0/00 as shown in Figure 8. The salinity determination on the second sample of the duplicate comparison was usually done 3-4 days after drawing the sample, while the first sample was run within one day. The average salinity difference of -.0017% indicates evaporation of the second salinity sample. All (CTD-Rosette) salinity comparisons were made against the first salinity determination.

Conductivity Cell Vertical Variation

The conductivity cell changes its dimensions with variations of temperature and pressure. As the conductivity cell changes its size the instrument measurement which is proportional to the conductance -G- will change.

$$G \propto \frac{R^2}{L} \quad (4)$$

$$G \propto \frac{R_o^2}{L_o} \frac{(1 + \frac{\Delta R}{R})^2}{(1 + \Delta L/L)} \quad (5)$$

where R_o and L_o are the unstressed cell condition and $\frac{\Delta L}{L}$ and $\frac{\Delta R}{R}$ are the coefficients of linear expansion for the conductivity cell. The cell material is assumed isotropic $\frac{\Delta R}{R} = \frac{\Delta L}{L}$. Neglecting second-order terms $(\frac{\Delta L_o}{L_o})^2$ the equations describing the conductance variation with cell dimensions reduces to:

$$G \propto \frac{R_o^2}{L_o} (1 + \Delta L/L) \quad (6)$$

The conductivity cell is made from Alumina (Al_2O_3). The coefficients of linear expansion given by General Electric for 99.9% pure Alumina at 20 °C are:

Temperature Dependence

$$\alpha = 6.5 \times 10^{-6} \text{ cm/cm/}^\circ\text{C}.$$

The bulk modulus of elasticity is given by Coors as 22.5×10^6 decibars which when converted to a linear compressibility yields:

Pressure Dependence

$$\beta = 1.5 \times 10^{-8} \text{ cm/cm/decibar .}$$

$$\frac{1}{22.5 \times 10^6 \times 3} = \beta$$

although how units change is unclear.

Since most of the world's ocean is colder at depth,

both temperature and pressure shrink the conductivity cell as the instrument descends. This cell deformation causes the conductivity to be underestimated by as much as .012 mmho/cm ($\sim .015$ 0/00) for a 5000 decibar station with a 20 °C temperature change.

The equation to correct the conductivity is:

$$\gamma = G * K (1 - \alpha(T - T_0) + \beta(P - P_0)) \quad (7)$$

G is the instrument conductivity

K is the cell factor at the reference pressure (P_0) and temperature (T_0).

Because of the stable deep water θ/S , the reference pressure and temperature for MODE data calibration was taken at 2.8 °C and 3000 decibars.

Figure 9 shows the distribution of salinity differences at various depths from the surface to 4500 decibars. The percentage of salinity differences between $\pm .003\%$ is given next to each

histogram. A linear compressibility value of β equals 5×10^{-8} cm/cm/decibars was used to obtain the CTD salinities. The material's compressibility may have yielded slightly better results since it would have reduced the surface CTD salinities roughly .002 0/00 while increasing the 4500 decibar CTD salinities by .001 0/00.

D. Down-Up Comparisons

Since laboratory calibration of CTD temperature was found not to depend on whether the electronics were immersed in the temperature bath, the CTD temperature forms a useful base for determining the down-up repeatability of the pressure and conductivity sensors. The pressure and salinity difference (down-up) at 17, 16.5, and 16 °C were computed for 21 stations. No lag correction was applied to the temperature (200 ms response) which for the average local temperature gradient of 10 m °C/decibar and lower rate of one decibar/sec amounts to approximately 4 m °C temperature difference between (down-up).

Oceanic-induced variations between down and up pressure or salinity values at selected isotherms are assumed to average to zero over enough stations while systematic differences in the pressure and conductivity measurement will not. The average pressure difference was found to be -1.0 decibars which means the pressure reads deeper on the way up. The pressure difference expected because of the temperature lag is + .4 decibars for the

10 m °C/decibars mean gradient. The standard deviation of the pressure differences is 7.4 decibars which is consistent with the isotherm depth scatter expected from internal waves.

Since the pressure sensor has reasonably good down-up repeatability, it is possible to use salinity difference to check the conductivity measurement for systematic errors. The average salinity difference is $-.004\%$ meaning the up salinity is salty. This difference is due to the lack of temperature lag correction before salinity computation.

II. TEMPERATURE LAG CORRECTIONS

A. Lag Correction Scheme

The Rosemount platinum wire temperature sensor has a nominal time constant of 200 msec. This is to be compared with the conductivity cells flushing time of about 30 msec. In order to calculate accurate salinities compensation must be made for the time constant discrepancy.

The time response of the temperature probe is assumed to be adequately described by a single equation of the form

$$\frac{dT}{dt} = \frac{1}{\tau} (T_o - T) \quad (8)$$

where T is the measured temperature, T_o is the true temperature, and τ is the time constant. This equation can be solved for the true temperature

$$T_o = T + \tau \frac{dT}{dt} . \quad (9)$$

Thus T_o can be estimated by finding the time derivative of the measured temperature series. Since the instrument records about six samples per time constant, some improvement of the response can be obtained by using Equation 9. However, due to the finite resolution of the digitizing circuit and possible electrical noise, the estimates of $\frac{dT}{dt}$ obtained from first differences are noisy. Thus

smoothing of the temperature series is desirable. This is accomplished by a least squares linear regression to estimate $\frac{dT}{dt}$.

For N data scans the temperature is assumed to be a linear function of time. The temperature at the n^{th} scan is

$$T_n = A t_n + b \quad (10)$$

where t_n is the time and A and B are obtained by a least squares regression to the N observations. For a sampling interval Δt , then the linear fit (10) can be written as

$$T_n = A \Delta t \times n + B$$

where n is the data scan number; $n = 1, \dots, N$. The estimate for the true temperature (Equation 9) now becomes

$$\begin{aligned} T_{on} &= A \Delta t n + B + A \tau \\ &= A \Delta t (n + n_L) + B \end{aligned} \quad (11)$$

where $n_L = \frac{\tau}{\Delta t}$, i.e., the time constant expressed in scans. Using standard least squares techniques, the coefficients are found to be

$$A \Delta t = \sum_{n=1}^N \frac{12n - 6(N+1)}{N(N^2-1)} T_n \quad (12)$$

$$B = \sum_{n=1}^N \frac{2(2N+1) - 6n}{N(N-1)} T_n \quad (13)$$

The mid point estimate at $\frac{N+1}{2}$ is

$$\bar{T} = \frac{1}{N} \sum_{n=1}^N T_n = B + \frac{N+1}{2} A \Delta t$$

$$\frac{dT}{dn} = A \Delta t.$$

Hence the estimate for the true midpoint temperature is

$$T_o = \bar{T} + A \Delta t n_L = \sum_{n=1}^N a_n T_n \quad (14)$$

where

$$a_n = \frac{1}{N} + n_L \frac{12n - 6(N+1)}{N(N^2-1)}; \quad \sum_{n=1}^N a_n = 1 \quad (15)$$

are the filter weights for the least squares smoothing.

This scheme allows the calculation of the true temperature at any time. The degree of smoothing of the measured temperature series is set by the number of points, N , used in the least squares regression.

B. Effect of Instrument Noise

If the measured temperature series contains random, uncorrelated noise, then the estimates of the true temperature, T_o , will also contain noise. Let the measured temperature be $T_n + \epsilon_n$ where ϵ_n is noise generated in the instrument after the temperature probe (e.g., digitizing noise). Then from (14) the calculated temperature will be

$$T_o = \sum_{n=1}^N a_n (T_n + \epsilon_n) = T_o' + \sum_{n=1}^N a_n \epsilon_n. \quad (16)$$

The variance of the noise in T_o over M samples is

$$\begin{aligned} \sigma^2 &= \frac{1}{M} \sum_{i=1}^M (T_{oi} - T_o')^2 = \frac{1}{M} \sum_{i=1}^M \left(\sum_{n=1}^N a_n \epsilon_{in} \right)^2 \\ &= \sum_{n=1}^N a_n^2 \sigma_\epsilon^2 \end{aligned} \quad (17)$$

where

$$\sigma_\epsilon^2 = \frac{1}{M} \sum_{i=1}^M \sum_{k=1}^M \epsilon_i \epsilon_k = \frac{1}{M} \sum_{i=1}^M \epsilon_i^2$$

assuming no correlation for the noise.

Thus, the ratio of the noise variance of the estimated temperature (T_o) to the noise variance of the measured temperature is

$$\begin{aligned} \frac{\sigma^2}{\sigma_\epsilon^2} &= \sum_{n=1}^N a_n^2 \\ &= \frac{1}{N} \left(1 + \frac{12 n_L^2}{N^2 - 1} \right). \end{aligned} \quad (18)$$

The noise in the estimated series increases rapidly with the magnitude of the lag n_L . For a lag $n_L = 6$ and $N = 3$, the noise ratio is 18.3.

This ratio is the total increase in noise. In the next section the frequency response of the correction scheme will be discussed. It will then be possible to consider the effect of the lag correction on the signal-to-noise ratio since this is the relevant parameter.

C. Frequency Response

The time lag in the temperature sensor attenuates high frequencies. This can be seen by expressing the temperature as a Fourier series of the form

$$T_o = \sum_{-\omega_Q}^{\omega_Q} \hat{T}_m^o e^{i\omega_m t} \quad (19)$$

where $\omega_Q = \frac{\pi}{\Delta t}$ is the Nyquist frequency. Expressing the measured temperature series in a similar expansion and substituting into Equation (9) gives:

$$\hat{T}_m^o = (1 + i \omega_m \tau) \hat{T}_m \quad (20)$$

Thus the spectral density ratio of the true temperature compared to the measured temperature is

$$\frac{\hat{T}_m^o \hat{T}_m^{o*}}{\hat{T}_m \hat{T}_m^*} = 1 + \omega_m^2 \tau^2 = 1 + \pi^2 n_L^2 \left(\frac{\omega_m}{\omega_Q}\right)^2 \quad (21)$$

This is the transfer function of the system.

In the absence of instrument noise Equation (20) gives the "ideal" correction scheme, i.e., Fourier transform the measured series, multiply each estimate by $(1 + i\omega \tau_m)$, and then perform an inverse Fourier transform to give the true temperature series as a function of time. The graph of the transfer function (21) is shown in Figure 11. At high frequencies the amplification becomes large.

Figures 10a and 10b show the spectra of the measured temperature series for a depth interval in the thermocline and deep water. The trend was removed from the data by first differencing the time series before calculating the spectrum. The spectra shown are recolored. The flattening of both these spectra is due to instrument noise. Note that the spectral level of the noise is the same in both cases, but the frequency at which the measured signal falls into the noise is different. This noise level is $.2 \times 10^{-7} \text{ } ^\circ\text{C}^2/\text{cycle}/\text{scan}$. Assuming white noise and integrating over the frequency bandwidth from 0 to ω_Q this corresponds to a total variance of $10^{-7} \text{ } ^\circ\text{C}^2$. The variance expected from the quantizing interval is

$$\sigma^2 = \frac{(\Delta T)^2}{12} \approx 2 \times 10^{-8} \text{ } ^\circ\text{C}^2.$$

Thus the measured temperature variance is five times the instrument quantizing noise. These measurements were made using a

prototype CTD. In later versions the additional noise has been eliminated by doubling the platinum thermometer resistance and using a times ten bridge (Brown, 1974).

Now consider the effect of applying the transfer function (Equation 21) or the spectral estimates in Figures 10a and 10b. For the lower frequencies where the real variance (the signal) is dominant, the transfer function increases both the signal and the noise. It leaves the signal-to-noise ratio constant. However, at the high frequencies the signal is buried in the noise. Here the transfer function is large and the noise amplification correspondingly large. Thus the signal-to-noise ratio integrated over all frequencies is changed by the lag correction, even though the ratio is unaffected at low frequencies. The dominance of noise at high frequencies suggests that a more appropriate correction transfer function would have a roll off at high frequencies.

The transfer function for the least square linear estimate is obtained from Equation 14 as follows:

$$\begin{aligned}
 T_o &= \sum_{n=1}^N a_n T_n \\
 &= \sum_{n=1}^N a_n \left(\sum_{\omega_m = -\omega_Q}^{\omega_Q} T_m \hat{e}^{i\omega_m (t_o + n\Delta t)} \right) \\
 &= \sum_{\omega_m = -\omega_Q}^{\omega_Q} \sum_{n=1}^N a_n e^{i\omega_m n\Delta T} \hat{T}_m e^{i\omega_m t_o} .
 \end{aligned}$$

Hence

$$R \equiv \frac{\hat{T}_m^* \hat{T}_m^O}{\hat{T}_m^* \hat{T}_m} = \left| \sum_{n=1}^N a_n e^{i\omega_m n \Delta t} \right|^2 \quad (22)$$

Letting

$$\delta = \frac{1}{2} \omega_m \Delta t = \frac{\pi}{2} \left(\frac{\omega_m}{\omega_Q} \right) \quad (23)$$

and

$$\phi(N, \delta) = \frac{\sin N\delta}{N \sin \delta} \quad (24)$$

then the sum in Equation (15) can be evaluated to yield

$$R(N, \delta) = \phi^2(N, \delta) + 9n_l^2 \left[\frac{\phi(N-1, \delta) - \phi(N+1, \delta)}{N \sin \delta} \right]^2 \quad (25)$$

for the transfer function.

The function $R(N, \delta)$ is plotted for three values of N in Figure 11. Also shown is the transfer function in Equation 21. Table 1 evaluates $R(N, \delta)$ for $N = 2, 5$. For $N = 2$ the transfer function of the least squares estimate (which in this case degenerates into the first difference estimate for dT/dt) closely follows the exact transfer function of the system. It provides no attenuation of the high frequencies. With $N = 3$, R follows Equation 21 for low frequencies but it does attenuate high frequencies. The higher N values produce a more complicated response function with more than one lobe.

The exact choice for N depends on the data being corrected. From Figure 10b it is clear that in the deep water one might choose a larger N than in the thermocline. However, the spectra only represent the average frequency content. An individual feature of interest could require more high frequencies for adequate resolution. For this reason $N = 3$ was chosen for the lag correction for all the data. If a further reduction in the high frequency response is desired, then a filter can be subsequently applied.

With the three-point correction the increase in the total noise is given by Equation 18. The instrument noise before the lag correction is assumed to have a flat frequency distribution. Its frequency distribution after the correction is given by (25) and is essentially the transfer function plotted in Figure 11. If the level of the noise is unacceptable, then it can be reduced by applying a low-pass filter. The frequency distribution will then be given by

$$R_T(\delta) = R(N, \delta) \cdot R_F(\delta) \quad (26)$$

where $R_F(\delta)$ is the transfer function of the filter. For an M point running mean

$$R_F(\delta, M) = \left| \frac{\sin(M\delta)}{M\delta} \right|^2 .$$

The total noise level is found by integrating the complete transfer function over all frequencies from 0 to ω_Q ($\delta = 0$ to $\delta = \frac{\pi}{2}$). It should be noted from Table 1 that for $N = 3$ the dominant contribution to the amplification comes from the term $n_L^2 \sin^2 2\delta = 36 \sin^2 2\delta$ for $n_L = 6$. In general only this term need be considered when estimating the noise increase. Table 2 gives specific examples of the total noise increase for the $N = 3$ lag correction followed by an M point running mean filter with $M = 2, 3, 4,$ and 5 .

D. Selecting the Temperature Probe Time Constant

In order to apply the above lag corrections it is necessary to know the instrument time constants accurately. The nominal value of 200 msec corresponds to 6.67 data scans. The true value could depend on a number of instrumental and operational parameters. Since no laboratory facility was available for measuring the time response, it was determined empirically from oceanic measurements.

The calculated salinity is sensitive to the lag correction. The true salinity is given by $S_o = S_o(T_o, C_o, P_o)$ where C_o and P_o are the true conductivity and pressure. The measured salinity is $S = S(T, C_o, P_o)$ assuming C_o and P_o are the measured values also. If no lag correction is made then the calculated salinity is consistently biased. For example, consider a constant temperature gradient of $-.030$ °C/meter. With the normal instrument lowering rate of 75 meters/min this corresponds to a temperature time

gradient of $-.038 \text{ }^\circ\text{C}/\text{sec} = -.00125 \text{ }^\circ\text{C}/\text{scan}$. If the time constant $\tau = 6$ scans, then $T - T_0 = .008 \text{ }^\circ\text{C}$. For reasonable temperatures ($15 \text{ }^\circ\text{C}$), conductivities (34 mmho/cm), and pressures (750 dbar) this temperature error yields a salinity which is about $.01 \text{ }^\circ/\text{oo}$ too fresh.

In addition to the salinity bias in a constant temperature gradient, the salinity will "spike" in regions with a sudden change in temperature gradient. If the instrument passes through a step where both T_0 and S_0 suddenly decrease, then the measured salinity will have a spike in the decreasing S direction. This happens since the measured temperature will be warmer than it should be while the measured conductivity will be nearly correct. Too warm a temperature combined with the correct conductivity yields too fresh a salinity.

Minimizing salinity spikes was used as the primary method for determining the time constant. Figure 12a shows a plot of T and C versus time in seconds and in scans for a section of data. The CTD digitizes a scan every 30 milliseconds. In Figure 12b the salinity is shown assuming several different temperature response times (n_L). In each case where $n_L \neq 0$ the $N = 3$ least squares lag correction was used. The salinity is extremely noisy for $n_L = 0$. The spikes are seen to correspond to the regions of large gradient. As n_L is increased from $n_L = 4$ scans to $n_L = 8$ scans, the sign of most of the spikes changes. While $n_L = 4$ scan is considerably better than $n_L = 0$, it still shows the salinity spikes. In the

range from $n_L = 5$ to $n_L = 7$ scans, the results are ambiguous. Some spikes change differently from others. This may indicate that the linear equation does not completely describe the temperature response. At $n_L = 8$ most of the spikes have reversed sign. This indicates too large a correction.

The result of these considerations is that $n_L = 6 \pm 1$ scan. Another method of deducing n_L was tried. The cross-spectrum of the measured temperature and conductivity should have a phase lag caused by the temperature-conductivity response time difference. This analysis did not yield results substantially different from the above. The discrimination among $\tau = 5, 6, \text{ or } 7$ scans was still ambiguous. In addition various combinations of τ_T (temperature) and τ_C (conductivity) were tried. Again the conclusion was that $\tau_C = 0$ and $n_L = 6 \pm 1$ scans were satisfactory.

The temperature response time was assumed to be $n_L = 6$ scans for all future work. The uncertainty of 1 scan in τ leads to a salinity uncertainty of about $.0015 \text{ }^\circ/\text{oo}$ in regions of large constant temperature gradient ($.030 \text{ }^\circ\text{C}/\text{meter}$). The error is smaller for smaller temperature gradients.

In order to complete the response time study the change of response time as a function of lowering rate was considered. The CTD was lowered through the main thermocline (600-800 dbar) at 30 m/min, 60 m/min, and 90 m/min. The response time was evaluated as described above. The results were essentially the same.

E. A Uniform Pressure Series and Error Estimates

The temperature lag correction requires the time sequence of measurements while data analysis of vertical profiles is done in terms of pressure. Before converting the lag corrected time series of P, T, and S to a uniform pressure series, the pressure is smoothed with a running mean filter with a half second averaging (15 scans) to interpolate missing pressure values. A uniform tenth decibar pressure series is then generated. The pressure is over-sampled with roughly two observations occurring for each pressure interval. The average of the measurements is computed for each interval.

Before lag correction and pressure sorting the observed instrument noise is $\sigma_T^2 = 10^{-7} \text{ } ^\circ\text{C}^2$ for temperature (see Section C) and $\sigma_C^2 = 8.7 \times 10^{-8} \text{ (mmho/cm)}^2$ for conductivity. This latter figure is equal to the noise level expected from the quantizing interval. Applying the temperature lag correction and the pressure sort yields an expected noise level (see Table 2) of $\sigma_T^2 = 10^{-6} \text{ } ^\circ\text{C}^2$. The lag correction program processes the conductivity in the same manner as the temperature; however, it sets the response time to $\tau_C = 0$. This results in an $N = 3$ scan running mean smoothing of the conductivity signal. Thus after pressure sorting $\sigma_C^2 = 1.6 \times 10^{-8} \text{ (mmho/cm)}^2$.

An accurate estimate of the salinity noise is difficult to achieve. Assuming that the above noise levels for temperature and

conductivity are independent, then we estimate a random noise level for salinity of $\sigma_S^2 \approx 2 \times 10^{-6} (\text{‰})^2$. In regions of large gradient fluctuations the salinity noise will be larger than this. However, this gives a rough estimate of the level.

Figures 13 and 14 show vertical wavenumber spectra of temperature for two depth intervals in the Sargasso Sea. These spectra were computed from the .1 decibar pressure sorted data. The linear trend was removed by first differencing prior to Fourier analysis. The spectra were subsequently recolored. In each figure spectra with and without lag correction are shown. In the thermocline, accurate representation of the high wave number variance requires the lag correction. However, in the deep water the variance reaches the instrument noise level at lower wavenumbers. The lag correction has little effect at these wavenumbers. The lag correction effect on the noise is pronounced. The structure observed at high wavenumbers is caused by the transfer function of the lag correction and of the pressure sorting acting on the original white noise. It is clear that as far as the average spectra properties are concerned there is no useful information in these higher wavenumbers in the deep water. They can be removed by additional filtering.

Figure 15 shows salinity spectra for the two depth intervals. The noise levels cut into the signal at lower wavenumbers than those seen in the temperature spectra. Again the noise dominates at high wavenumbers in the deep water.

III. THE SALINITY ALGORITHM

The CTD sensors yield temperature T ($^{\circ}\text{C}$), pressure P (decibars) and conductivity C (mmho/cm) using calibrations for the individual sensors. For example, a reading G from the conductivity sensor might be related to the conductivity by

$$C(T,S,P) = KG \quad (27)$$

where K is the cell factor (see the conductivity calibration section for a detailed discussion). The problem is to invert Equation (27) to yield

$$S = S(T,C,P). \quad (28)$$

A. Temperature Conversion

The CTD has been calibrated to the 1968 International Practical Temperature Standard (IPTS) while all of the conductivity ratios used in the salinity algorithm were developed on the 1948 IPTS. The difference between the 1948 IPTS and 1968 IPTS can be closely approximated by the quadratic equation. The choice of constants for the fit give best results in the range 0 to 30 $^{\circ}\text{C}$. In order to make the CTD temperature coincide with the 1948 IPTS for salinity computations, and internal temperature conversion of the following form is applied to temperature.

$$T = T_{68} + 4.4 \times 10^{-6} T_{68} (100 - T_{68}) \quad (29)$$

T is the equivalent 1948 IPTS CTD temperature °C

T_{68} is the 1968 IPTS CTD temperature °C.

B. Conductivity Ratios

Because conductivity is difficult to measure in absolute units, most investigators have worked with conductivity ratios.

The appropriate ratios are defined below.

The basic measurement of conductivity is expressed as the ratio

$$\begin{aligned} R &= C(T,S,P)/C(15,35,0) \\ &= \frac{K}{C(15,35,0)} G = kG \end{aligned} \quad (30)$$

where k is a modified calibration constant to yield the ratio.

Knowles tabulated values of electrical conductivity of sea water at 15 °C, 35 ‰, and atmospheric pressure determined from various investigations. The average of the values he obtains for Reeburgh's data gives a value of 42.909 mmho/cm for C(15, 35,0).

Brown and Allentoft (1966) have determined the ratio

$$R_T = C(T,35,0)/C(15,35,0) \quad (31)$$

as a polynomial in temperature (see Appendix I). These determinations were made at atmospheric pressure, denoted in the equations by P = 0.

The ratio

$$R_S = C(T, S, 0) / C(T, 35, 0) \quad (32)$$

is given in the International Oceanographic Tables published by the National Institute of Oceanography (U.K.) and UNESCO. The notation used in the tables is R_T for the ratio. The change to R_S in the present report is made to unify the notation for the various ratios used.

The empirical formulas published in the tables relate the ratio R_S to the salinity as follows:

$$S = S(R_{15}); \quad R_{15} = C(15, S, 0) / C(15, 35, 0) \quad (33)$$

(a polynomial in R_{15}), and

$$R_{15} = R_{15}(T, R_S) \quad (34)$$

a polynomial in temperature and R_S . The two empirical formulas together define the function

$$S = S(R_{15}(T, R_S)) = S(T, R_S). \quad (35)$$

Schleicher and Bradshaw (1965) have determined the ratio

$$R_P = C(T, S, P) / C(T, S, 0) \quad (36)$$

as a polynomial in temperature, salinity, and pressure.

The four ratios are related by the identity

$$R = R_T R_S R_P. \quad (37)$$

Given R , T , and P , the problem is to evaluate R_T and R_P so that R_S can be calculated. The values of T and R_S are then substituted into (35) to evaluate salinity S .

C. Computational Procedure

Given the conductivity ratio R , temperature T , and pressure P , identity (37) is inverted to yield

$$R_S = R/R_T R_P .$$

The ratio R_T is a function of temperature only and can be evaluated directly. However, the ratio R_P depends on salinity and cannot be evaluated explicitly. The dependence is weak and it is possible to use an iterative process to evaluate salinity. An initial value S^0 is assumed, (i.e., $S^0 = 35$ ‰, initial guess) to estimate R_P^0 , i.e.,

$$R_P^0 = R_P(T, S^0, P) \quad (38)$$

which, in turn, yields the estimates

$$R_S^0 = R/R_T R_P^0 \quad (39)$$

$$S^1 = S(T, R_S^0) .$$

The corrected value S^1 is substituted into equation (38) to yield R_P^1 , R_S^1 , and S^2 . The cycle is repeated until the difference of

salinity estimates, $S^{n+1} - S^n$, is acceptably small (.005 ‰ gives a negligibly small error).

SUMMARY

The W.H.O.I./Brown CTD gives data equal to or better than the best hydrography stations data. The accuracy achieved during MODE was: temperature ± 0.0015 °C; pressure ± 1.5 decibars, and salinity ± 0.003 ‰. Good laboratory calibrations of temperature and pressure are necessary to achieve such results and a constant monitoring of conductivity at sea is required to obtain this salinity accuracy. No hysteresis between down and up profiles is evident in pressure or conductivity.

Our best estimation of the Rosemount temperature response time is 6 ± 1 scan or 180 ± 30 milliseconds. The temperature series is corrected for this lag by a centered three-point least squares regression to the temperature time series. Estimates for random noise in the raw measurements are: temperature $\sigma_T^2 = 10^{-7} (\text{°C})^2$; conductivity $\sigma_C^2 = 8.7 \times 10^{-8} (\text{mmho/cm})^2$. The noise estimates for .1 decibar uniform pressure series are: temperature - $\sigma_T^2 = 10^{-6} (\text{°C})^2$. Systematic errors in salinity due to uncertainties in the temperature time constant amount to ± 0.001 ‰ in the main thermocline.

The salinity algorithm developed appears to work reasonably well although the temperature range of the data on which the equation for R_{15} was developed doesn't extend to the low temperatures in situ measurements require.

APPENDIX I

EMPIRICAL FORMULAS1. Conductivity Ratio R_T

$$R_T = C(T, 35, 0) / C(15, 35, 0)$$

$$= \sum R_{Tn} T^n$$

$$R_{T0} = +0.67652453$$

$$R_{T1} = +0.20131661 \times 10^{-1}$$

$$R_{T2} = +0.99886585 \times 10^{-4}$$

$$R_{T3} = -0.19426015 \times 10^{-6}$$

$$R_{T4} = -0.67249142 \times 10^{-8}$$

Range of Validity

$$R_T \sim 0.67 - 1.48$$

$$T \sim 0 - 35 \text{ } ^\circ\text{C}$$

$$S \sim 35 \text{ } ^\circ\text{/}\text{oo (standard sea water)}$$

$$P \sim 1 \text{ atmosphere}$$

Accuracy of Determination

$$T \sim \pm 0.003 \text{ } ^\circ\text{C}$$

$$R_T \sim \pm 0.00013$$

$$\text{Formula} \sim \pm 0.00004$$

2. Conductivity Ratios R_{15} and R_S

$$R_{15} = C(15, S, 0) / C(15, 35, 0)$$

$$R_S = C(T, S, 0) / C(T, 35, 0)$$

$$R_{15} = R_S + 10^{-5} [R_S (R_S - 1) (T - 15)] [96.7 - 72.0 R_S + 37.3 R_S^2 - (0.63 + 0.21 R_S^2) (T - 15)]$$

Range of Validity

$$T \sim 14 - 29 \text{ }^\circ\text{C}$$

$$R_S \sim 0.85 - 1.19$$

Accuracy of Determination

T not given

$$R_{15} \sim 9 \times 10^{-5} \text{ (uncertainty)}$$

$$R_S \sim 0.05 \Delta_{15} = 0.05 (R_{15} - R_S)$$

$$\sim \pm 9 \times 10^{-5}$$

(International Oceanographic
Tables, 1966)

3. Salinity

$$S = S(R_{15})$$

$$= \sum S_n R_{15}^n$$

$$S_0 = -0.08996$$

$$S_1 = +28.29720$$

$$S_2 = +12.80832$$

$$S_3 = -10.67869$$

$$S_4 = +5.98624$$

$$S_5 = -1.32311$$

Range of Validity

$$S \sim 4 - 42 \text{ } ^\circ/\text{oo}$$

$$R_{15} \sim .10 - 1.19$$

Accuracy of Determination

$$S \sim .002 \text{ } ^\circ/\text{oo} \quad \text{Repeatability}$$

$$R_{15} \sim 9 \times 10^{-5} \quad \text{Uncertainty}$$

4. Conductivity Ratio R_p

$$R_p = C(T,S,P)/C(T,S,O)$$

$$R_p = 1 + 10^{-2} [g(T)f(P) + h(P)j(T)] [1 + l(T)m(S)]$$

$$g(T) = \sum g_n T^n$$

$$f(P) = \sum f_n P^n$$

$$h(P) = \sum h_n P^n$$

$$j(T) = \sum j_n T^n$$

$$l(T) = \sum l_n T^n$$

$$m(S) = 35 - S$$

n	g_n	f_n	h_n	j_n	l_n
0	+1.5192	0	+4.0 10^{-4}	+1.000	+6.950 10^{-3}
1	-4.5302 10^{-2}	+1.04200 10^{-3}	+2.577 10^{-5}	-1.535 10^{-1}	-7.6 10^{-5}
2	+8.3089 10^{-4}	-3.3913 10^{-8}	-2.492 10^{-9}	+8.276 10^{-3}	
3	-7.900 10^{-6}	+3.300 10^{-13}		-1.657 10^{-4}	
	$^{\circ}\text{C}$	decibars	decibars	$^{\circ}\text{C}$	$^{\circ}\text{C}$

Range of Validity

$$T \sim 0 - 25 \text{ } ^{\circ}\text{C}$$

$$P \sim 0 - 10,000 \text{ db}$$

$$S \sim 31 - 39 \text{ } ^{\circ}/\text{oo}$$

$$R_p \sim 1.000 - 1.115$$

Accuracy of Determination

$$\pm 0.001 \text{ } ^{\circ}\text{C}$$

$$\pm 1 \text{ db}$$

$$\pm 0.01 \text{ } ^{\circ}/\text{oo}$$

(Bradshaw-Schleicher, 1965)

APPENDIX II

CONDUCTIVITY CALIBRATION TECHNIQUE

The conductivity calibration is obtained from salinity either collected during a station or historical data. The problem is to determine the conductivity adjustment from a salinity offset. A value of $\partial C/\partial S$ is necessary to convert ΔS to ΔC , but $\partial C/\partial S$ varies with temperature, pressure, and salinity making tabulation, graphs or a function necessary. A $\partial C/\partial S$ change of 1 part in 10^3 introduces conductivity error roughly .0001 mmho/cm (\sim .0001 ppt) for an initial salinity error ΔS of .1 ppt.

The procedure is as follows:

$$\Delta S = S_{\text{Standard}} - S_{\text{CTD}}$$

ΔS is the change in salinity.

S_{Standard} is obtained from water sample or historic data.

$$\Delta C = \Delta S \left. \frac{\partial c}{\partial s} \right|_{T, P, \bar{S}}$$

ΔC is the change in conductivity.

T is the CTD temperature.

P is the CTD pressure.

$$\bar{S} = (S_{\text{CTD}} + S_{\text{True}})/2$$

$\frac{\partial c}{\partial s}$ read to the nearest thousandth

The Cell Factor (C.F.) multiplies the CTD conductivity to obtain the true conductivity.

$$\text{C.F.} = \frac{C_{\text{CTD}} + \Delta C}{C_{\text{CTD}}}$$

The W.H.O.I. CTD data logging program AQUIS provides a listing of the variables necessary to find the appropriate $\partial C/\partial S$ (i.e., P,T,S); plus potential temperature to obtain a historic salinity value and the initial CTD conductivity for computing the cell factor. This conductivity calibration technique requires calibrated temperature and pressure be used in the listing.

Because the temperature and salinity at any depth varies over the world oceans, graphs or an equation appropriate to specific ocean regions are necessary. A least squares linear regression for $\partial C/\partial S$ good for deep water calibration over much of the world's oceans

$$\left. \frac{\partial C}{\partial S} \right| = .790 + 2.2 \times 10^{-2} (T-1.0) + 6.9 \times 10^{-6} (P-2400) \\ + 3.75 \times 10^{-3} (35-S)$$

Range T - 1.0 - 3.1 °C

P - 2400 - 4200 dbars

S - 34.7 - 35.5 ‰

For the MODE data a historic potential temperature-salinity relationship developed by Crease (Ref. MODE Density Manual) was used to calibrate the CTD. The curve is tabulated together with the Worthington-Metcalf θ/S for comparison.

The CTD-computed potential temperature depends weakly on salinity. A .1 ppt error in salinity will yield a .0005 °C error in potential temperature. For the Crease θ/S relationship, the result is a 5×10^{-5} ppt error in salinity.

HISTORIC POTENTIAL TEMPERATURE-SALINITY
RELATIONSHIPS FOR THE WESTERN
NORTH ATLANTIC

θ	S_{Crease}	$S_{\text{Worthington-Metcalf}}$
2.05	34.913	34.914
2.10	.916	.917
2.15	.919	.919
2.20	.921	.922
2.25	.924	.925
2.30	.927	.928
2.35	.930	.931
2.40	.933	.934
2.45	.936	.936
2.50	.938	.939
2.55	.941	.942

REFERENCES

- Boyce, Farrell M., 1966. A Brief Study of the Accuracy of the Protected Deep-Sea Reversing Thermometer. Fisheries Research Board of Canada, Manuscript #227.
- Bradshaw, A. and K. E. Schleicher, 1965. The effect of pressure on electrical conductance of sea water. Deep-Sea Res. 12 151-162.
- Brown, N. and B. Allentoft, 1966. Salinity, conductivity and temperature relationships of sea water over the range of 0 to 60 p.p.t. Bissett-Berman Corp., Manuscript Report. March 1, 1966.
- Brown, Neil, 1974. A Precision CTD Microprofiler, Proceedings IEEE International Conference on Engineering in the Ocean Environment.
- Cox, R. A., F. Culkins, and J. P. Riley, 1967. The electrical conductivity/chlorinity relationship in natural sea water for $S = S(R_{15})$, Deep-Sea Res. 14, 203-220.
- Cross, J. L., 1963. Reduction of Data for Piston Gauge Pressure Measurements. U. S. Department of Commerce, National Bureau of Standards, Monograph 65.
- International Oceanographic Tables, 1966. National Institute of Oceanography (U.K.) and UNESCO.
- The International Practical Temperature Scale of 1968 Adopted by Cmite' International des Poids et Mesures. International Journal of Scientific Metrology, 5, No. 2, April 1969, pp. 35-44.
- Johnson, D. P. and D. H. Newhall, 1953. The Piston Gauge as a Precise Measuring Instrument. Transactions of the ASME, 75, pp. 301-310.
- Knowles, C. E., 1974. Salinity determination from use of CTD sensors, Journal of Physical Oceanography 4, 275-277.
- Platinum Resistance Thermometry. U. S. Department of Commerce, National Bureau of Standards, Monograph 126. April 1973.
- Reeburgh, W. S., 1965. Measurements of the electrical conductivity of sea water. Journal of Marine Research 23, 187-199.

Whitney, G. G., Jr., 1957. Factors Affecting the Accuracy of Thermometric Depth Determinations. *Extrait du Journal Conseil Purl'Explication de la Mer*, 12, 167-173.

Worthington, L. V., W. G. Metcalf, 1961. The Relationship between Potential Temperature and Salinity in Deep Atlantic Water. *Papp. et Proc.-Verb Vol. 149, Cons. Internat. Explor. de la Mer*.

Wright, W. R. and L. V. Worthington, 1970. The Water Masses of the North Atlantic Ocean: A Volumetric Census of Temperature and Salinity. *Folio 19. American Geographical Society*.

W.H.O.I./Brown CTD Microprofiler

Figure Captions

- Fig. 1. Temperature correction graph for CTD. Includes six calibrations over a 16 month period.
- Fig. 2. Distribution of 175 temperature comparisons between deep-sea reversing thermometers and the corrected CTD temperature for temperatures less than 4.5°C , $\overline{\Delta T} = -.5\text{m}^{\circ}\text{C}$, $\sigma_{\Delta T} = 10 \text{ m}^{\circ}\text{C}$.
- Fig. 3. Pressure correction graphs for the CTD. Includes piston gage - CTD (Δ), average CTD difference from thermometric pressure (\bullet), and calibration curve adopted for MODE.
- Fig. 4. Distribution of 189 pressure comparisons between unprotected reversing thermometers and the uncorrected CTD pressure. $\overline{\Delta P} = -1.7$ decibars.
- Fig. 5. Deep-water potential temperature-salinity diagram with MODE water sample salinities indicated as dots. Average potential temperature salinity curves by Crease, Worthington-Metcalf, and Worthington-Wright are shown for comparison.
- Fig. 6. Cell factor time variations during MODE. Noisy stations during June 1973 are calibrated to individual station water samples.
- Fig. 7. Distribution of 269 salinity comparisons between water samples and the corrected CTD salinities over zero to 4500 decibar pressure range.

- Fig. 8. Distribution of 208 salinity comparisons from duplicate water samples left standing several days and first thermostatic salinometer determination. $\Delta\bar{S} = -.0018 \text{ }^{\circ}/\text{oo}$; $\sigma_s = .003 \text{ }^{\circ}/\text{oo}$.
- Fig. 9. Distribution of 269 salinity comparisons from water samples and the corrected CTD, broken down by pressure level. The percentage of the observations between $\pm .003 \text{ }^{\circ}/\text{oo}$ is given for each level.
- Fig. 10. Frequency spectra $F_T(f)$ for the measured temperature series in terms of cycles/scan. (a) Main thermocline data (600-800 m depth), (b) North Atlantic Deep Water data (2600-2800 m depth).
- Fig. 11. The transfer function for the least squares lag correction schemes using 2, 3, and 5 points. Also shown is the transfer functions defined by Equation 21.
- Fig. 12. (a) Time series of temperature, T, and conductivity, C, for a section of a lowering. (b) The time series for the salinity calculated from the data in 12a using a three point (N=3) lag correction scheme and a temperature time lag n_L as noted.
- Fig. 13. Vertical wave number spectrum $F_T(k)$ of temperature observed in the main thermocline (600-800 decibars). The solid line is before lag correction. The dashed line is after lag correction.

Fig. 14. Vertical wave number spectrum $F_T(k)$ of temperature observed in the North Atlantic Deep Water (2600-2800 decibars). The solid line is before lag correction. The dashed line is after lag correction.

Fig. 15. Vertical wave number spectrum $F_S(k)$ of salinity observed in the two depth interval indicated. The temperature data were lag corrected prior to calculating the salinity.

Table Captions

Table 1. The transfer function, $R(N, \delta)$, for the least squares lag correction. $N = 2,5 - \delta = \pi/2 (\omega_m / \omega_Q)$.

Table 2. Increase in the instrument noise level (variance) for a three point lag correction followed by an M point running mean filter.

Table 1

THE TRANSFER FUNCTION, $R(N, \delta)$, FOR THE LEAST SQUARES LAG CORRECTION. $N = 2, 5$

$$\delta = \frac{\pi}{2} \left(\frac{\omega_m}{\omega_Q} \right)$$

$$N = 2 \quad R(2, \delta) = \cos^2 \delta + 4n_L^2 \sin^2 \delta$$

$$N = 3 \quad R(3, \delta) = 1 - \frac{8}{3} \sin^2 \delta + \frac{16}{9} \sin^4 \delta + n_L^2 \sin^2 2\delta$$

$$N = 4 \quad R(4, \delta) = \cos^2 \delta (1 - 2 \sin^2 \delta)^2 + 4n_L^2 \sin^2 \delta (1 - \frac{6}{5} \sin^2 \delta)^2$$

$$N = 5 \quad R(5, \delta) = (1 - 4 \sin^2 \delta + \frac{16}{5} \sin^4 \delta)^2 + n_L^2 \sin^2 2\delta (1 - \frac{8}{5} \sin^2 \delta)^2$$

Table 2

INCREASE IN THE INSTRUMENT NOISE LEVEL (VARIANCE)
FOR A THREE POINT LAG CORRECTION FOLLOWED
BY AN M POINT RUNNING MEAN FILTER

M	σ^2/σ_o^2
2	8
3	4
4	2
5	1.5

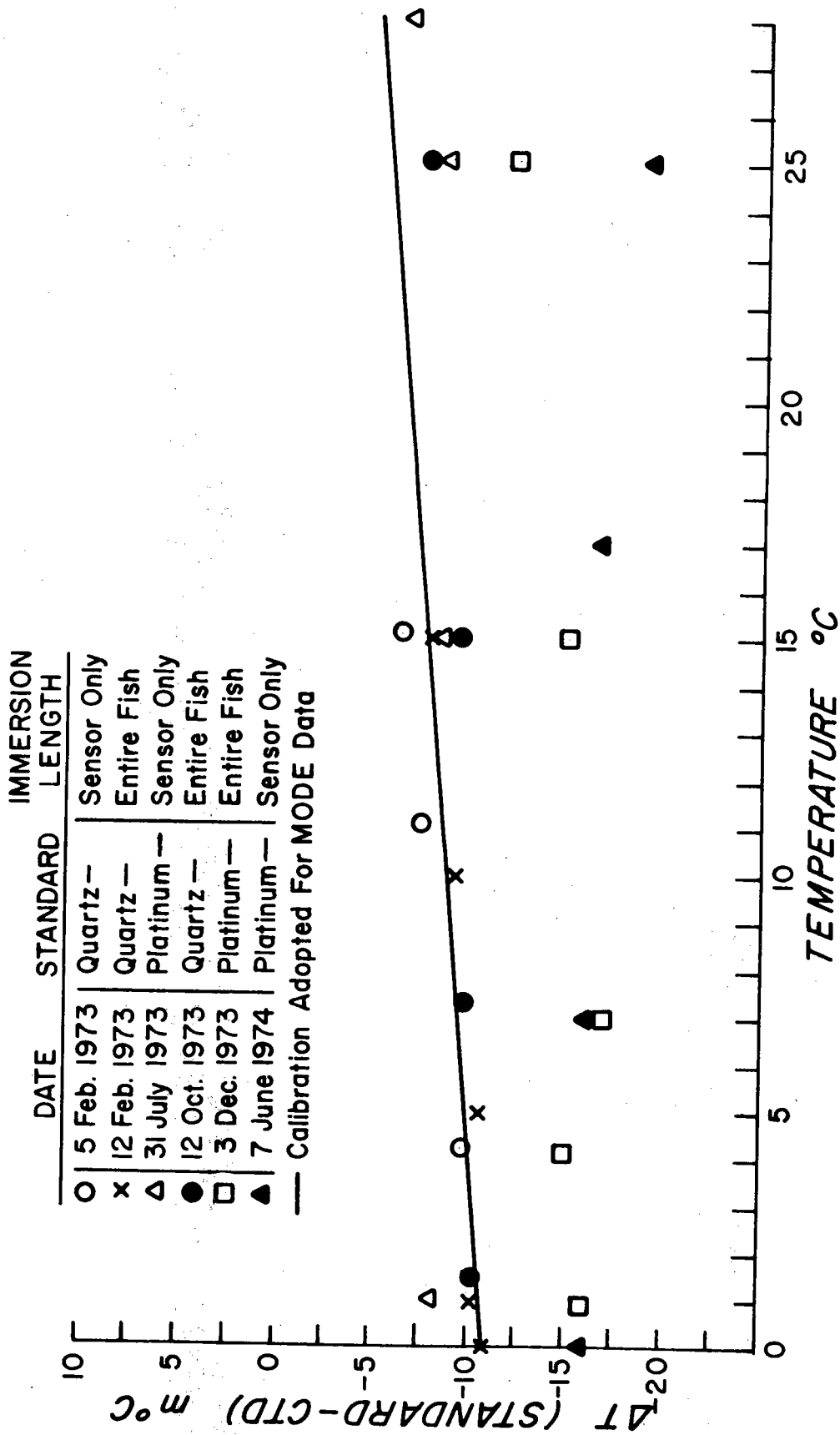


Figure 1.

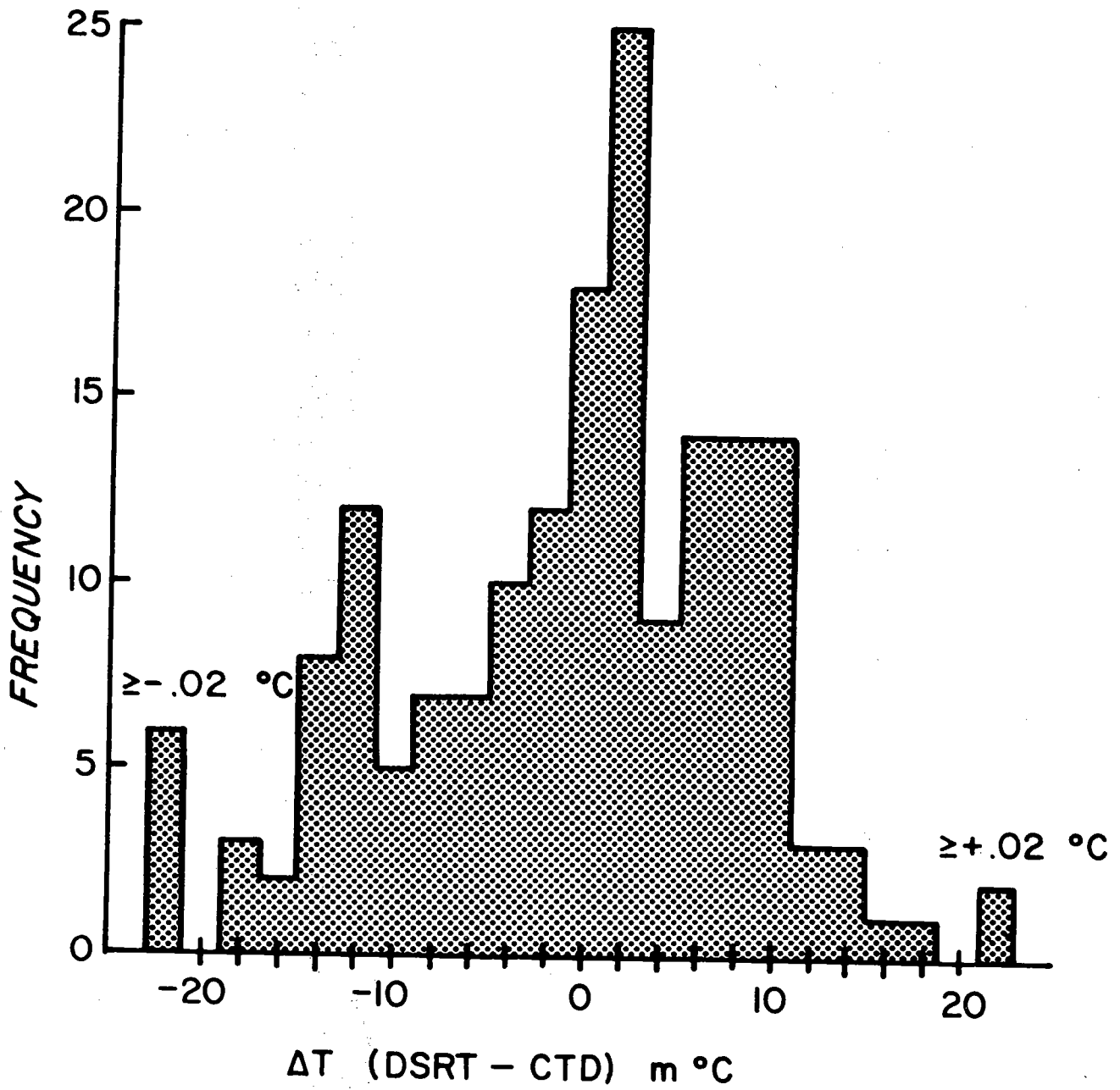


Figure 2.

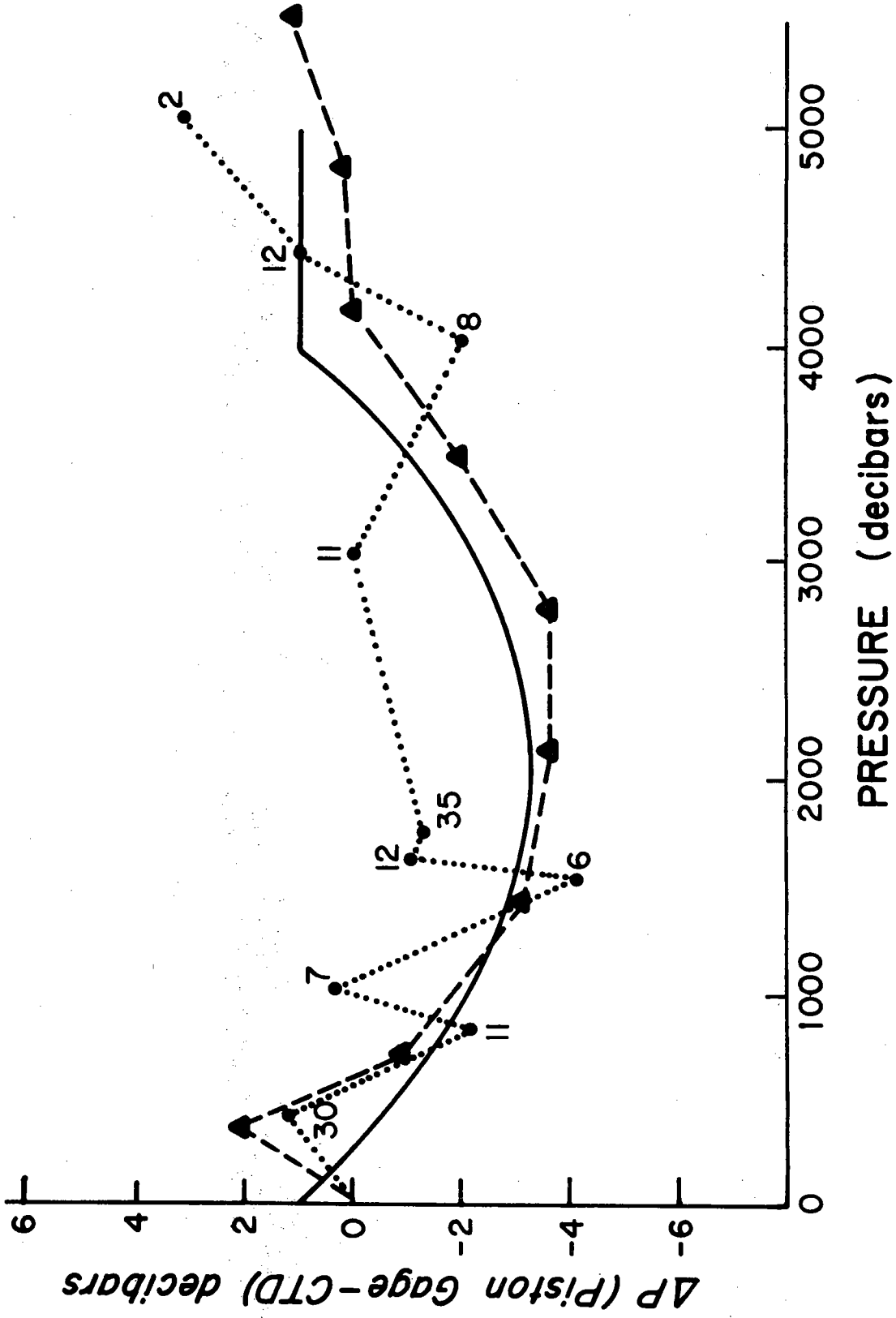


Figure 3.

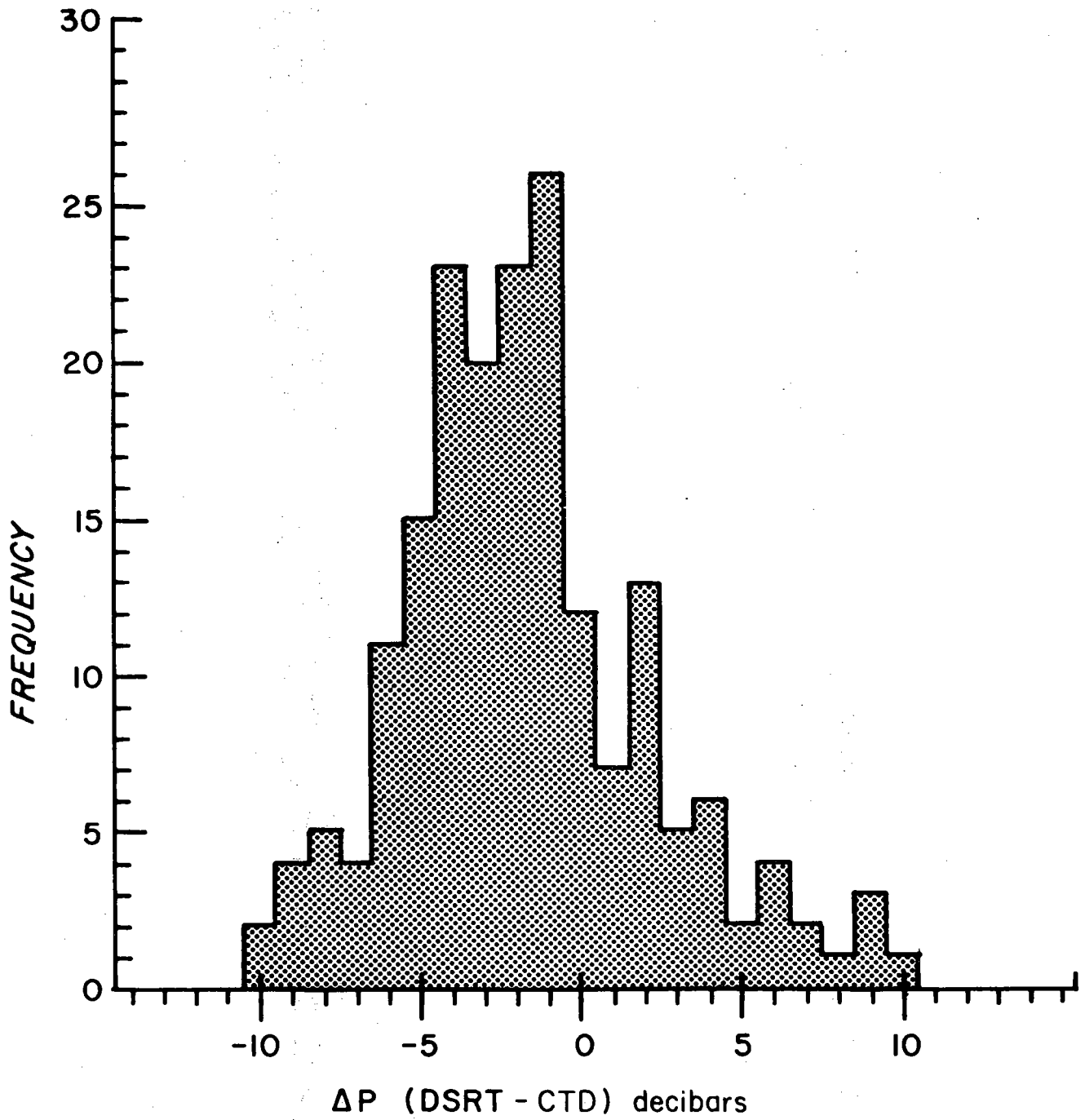


Figure 4.

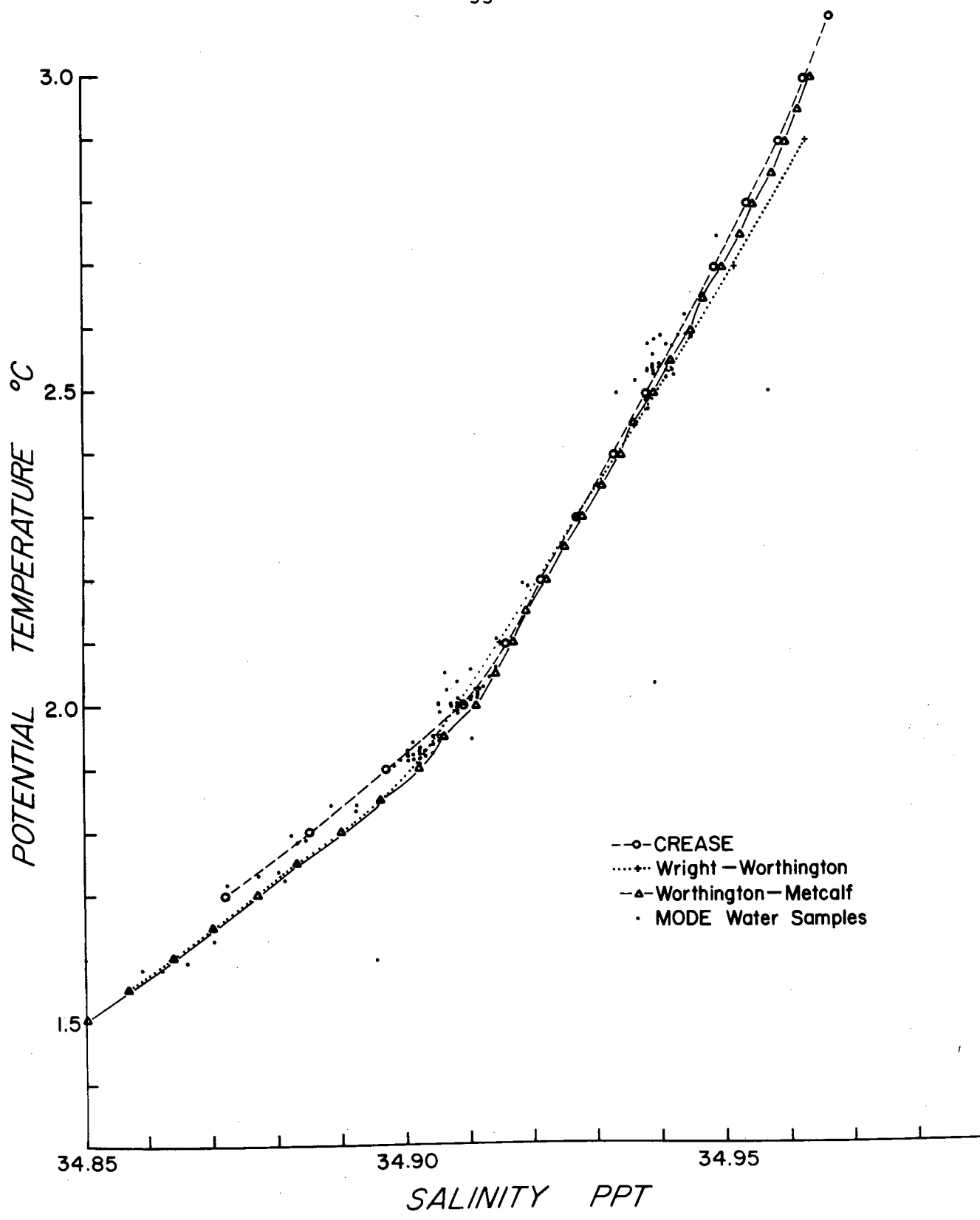


Figure 5.

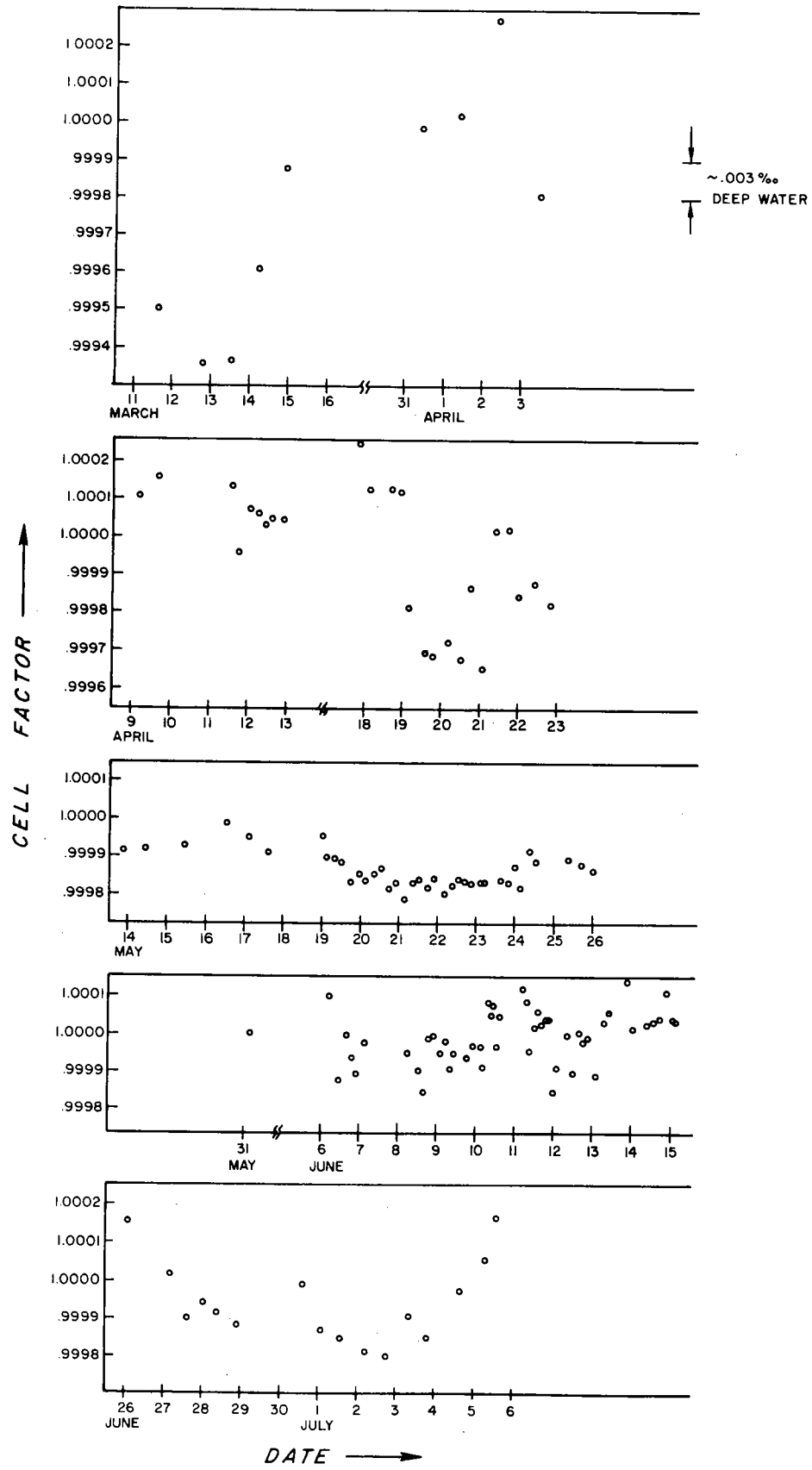


Figure 6.

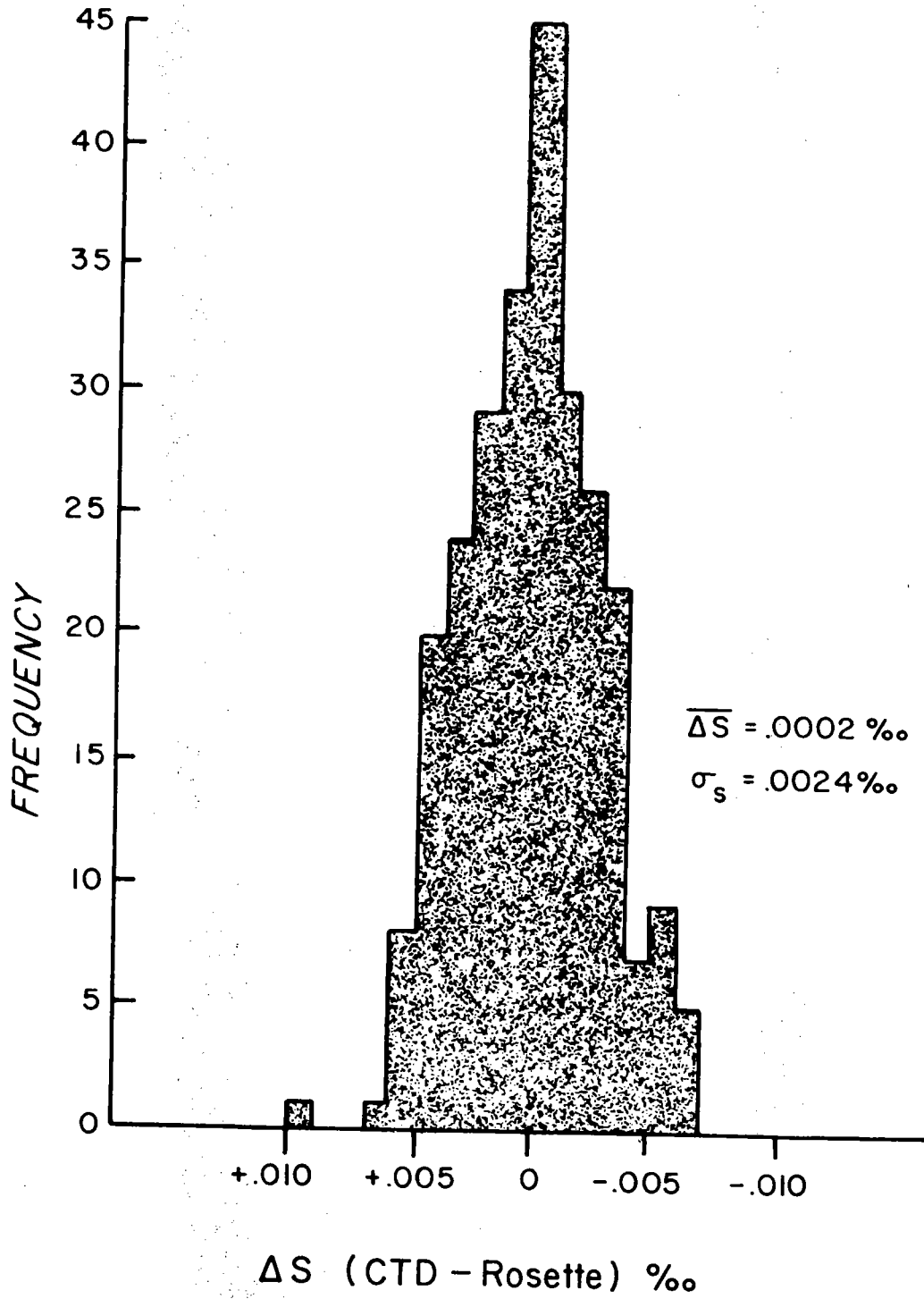


Figure 7.

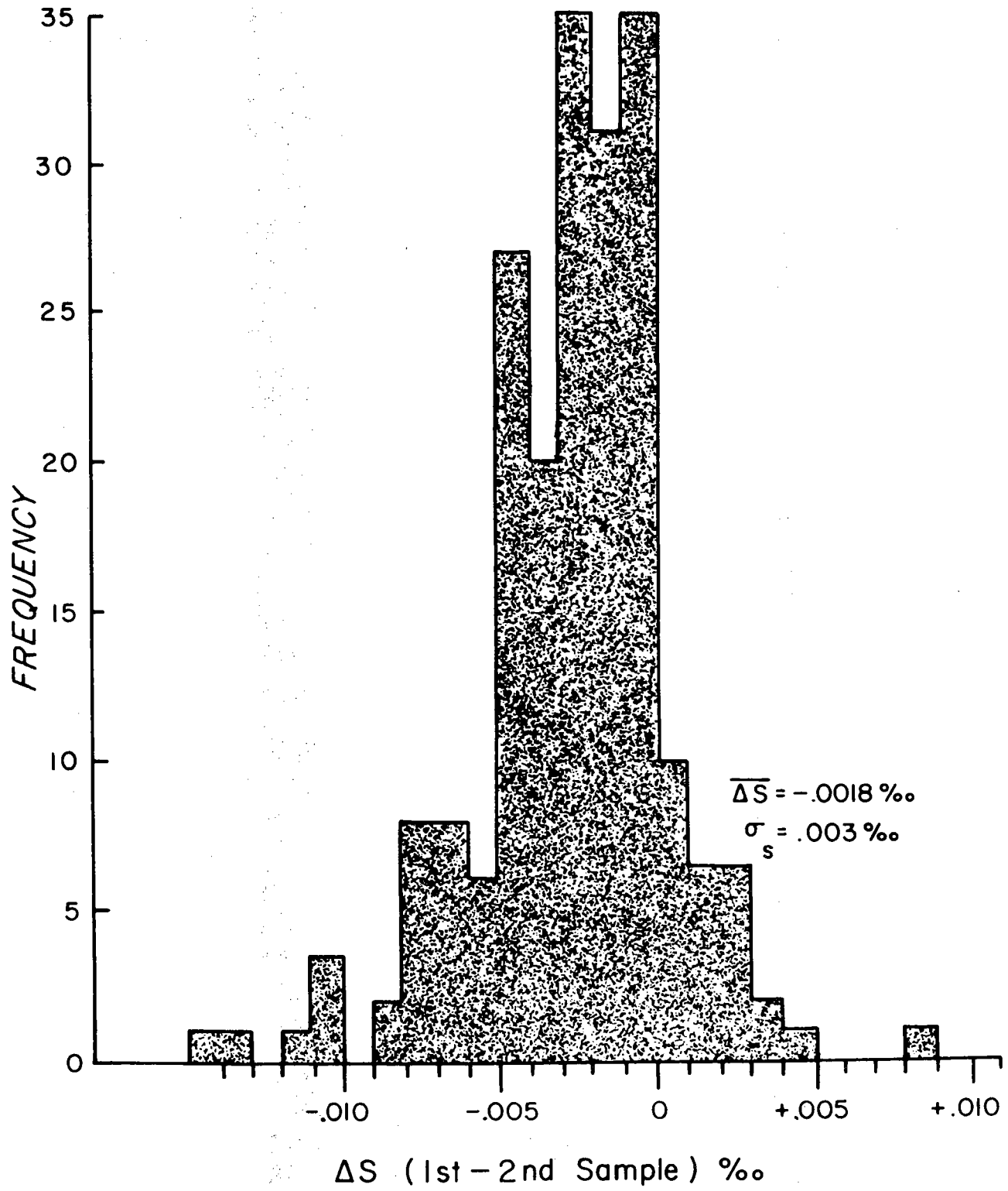


Figure 8.

SALINITY DIFFERENCES (%) CTD - ROSETTE
 (62 STATIONS R.V. CHAIN CRUISE 112)

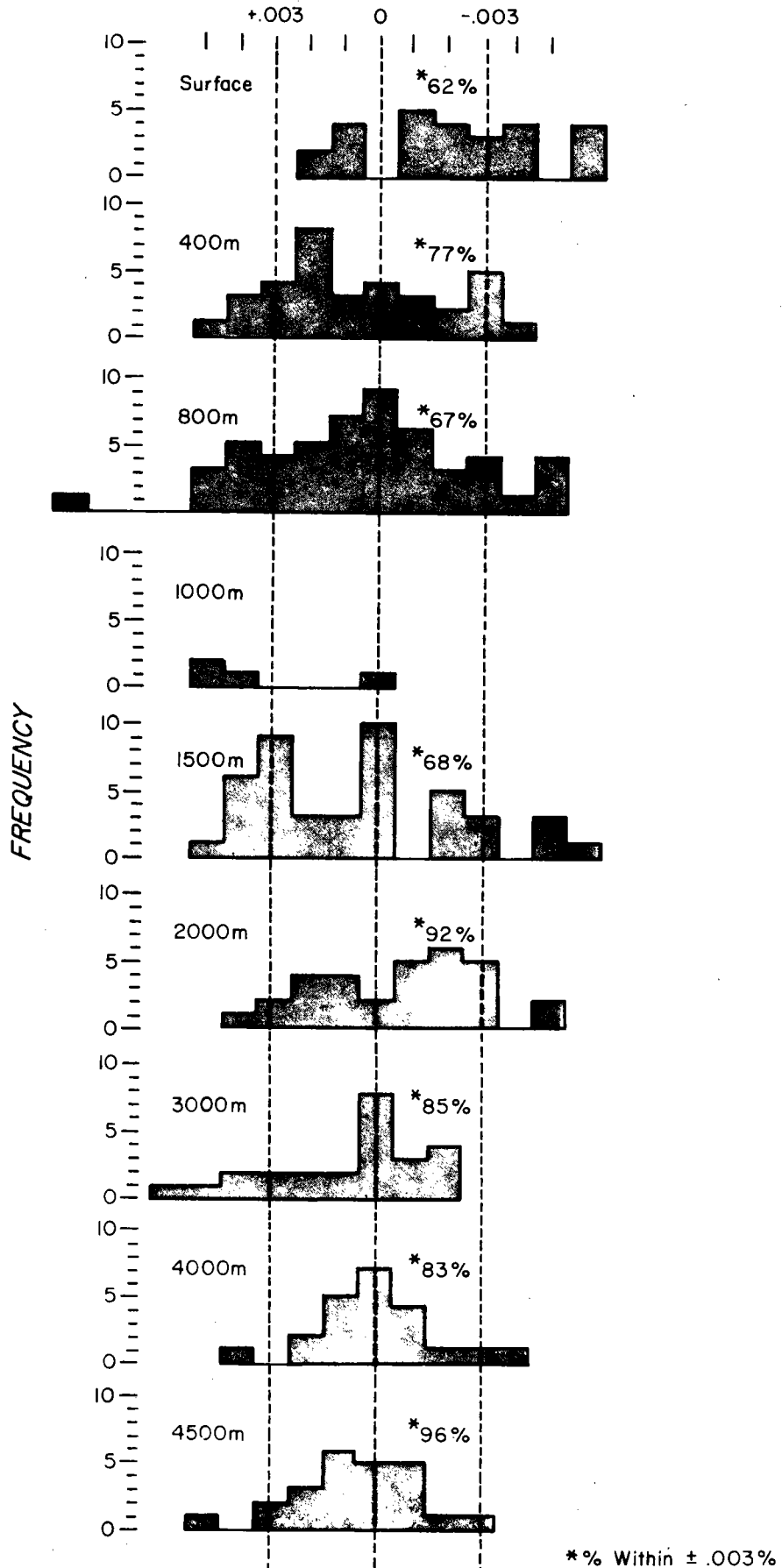


Figure 9.

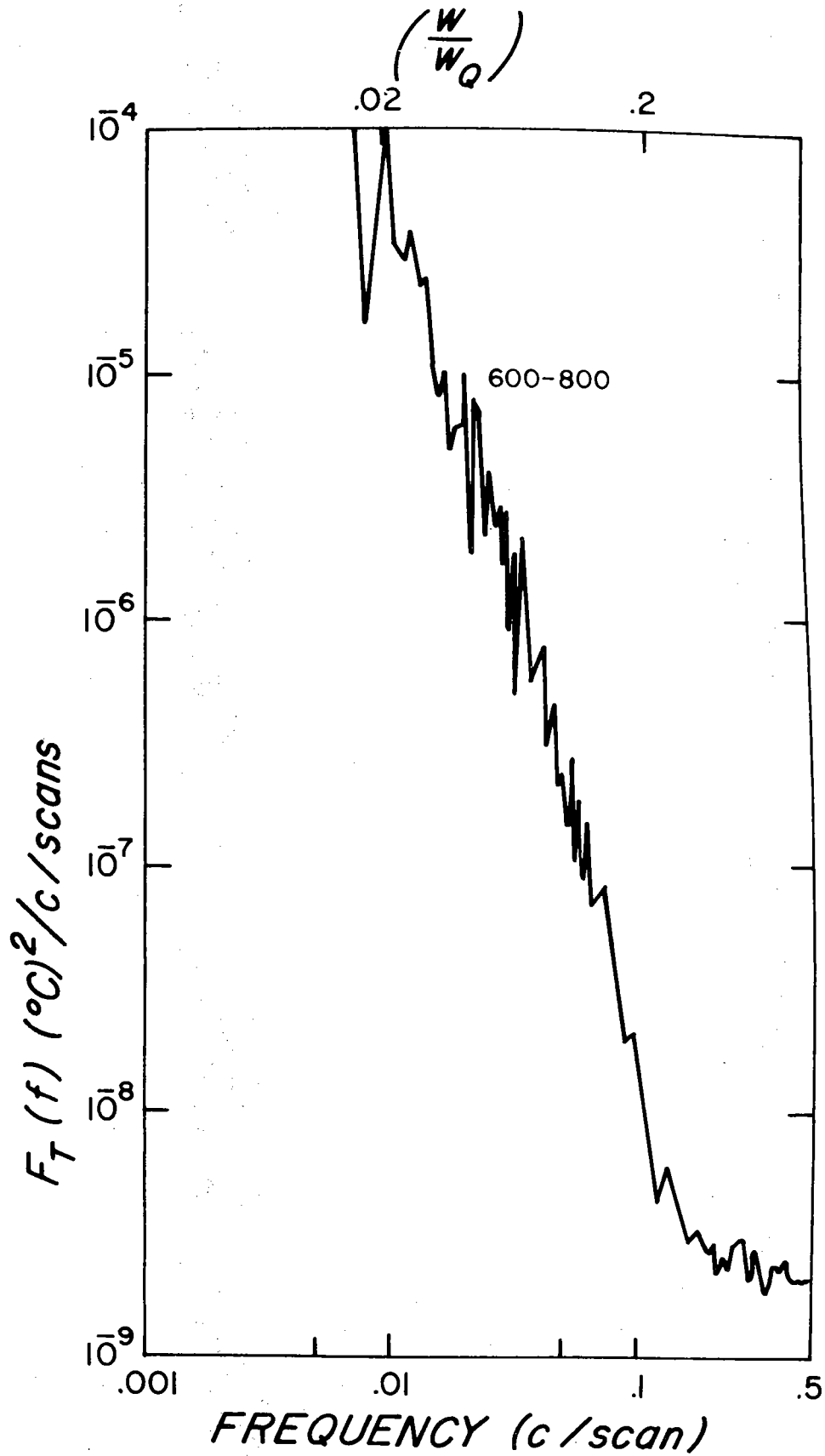


Figure 10a.

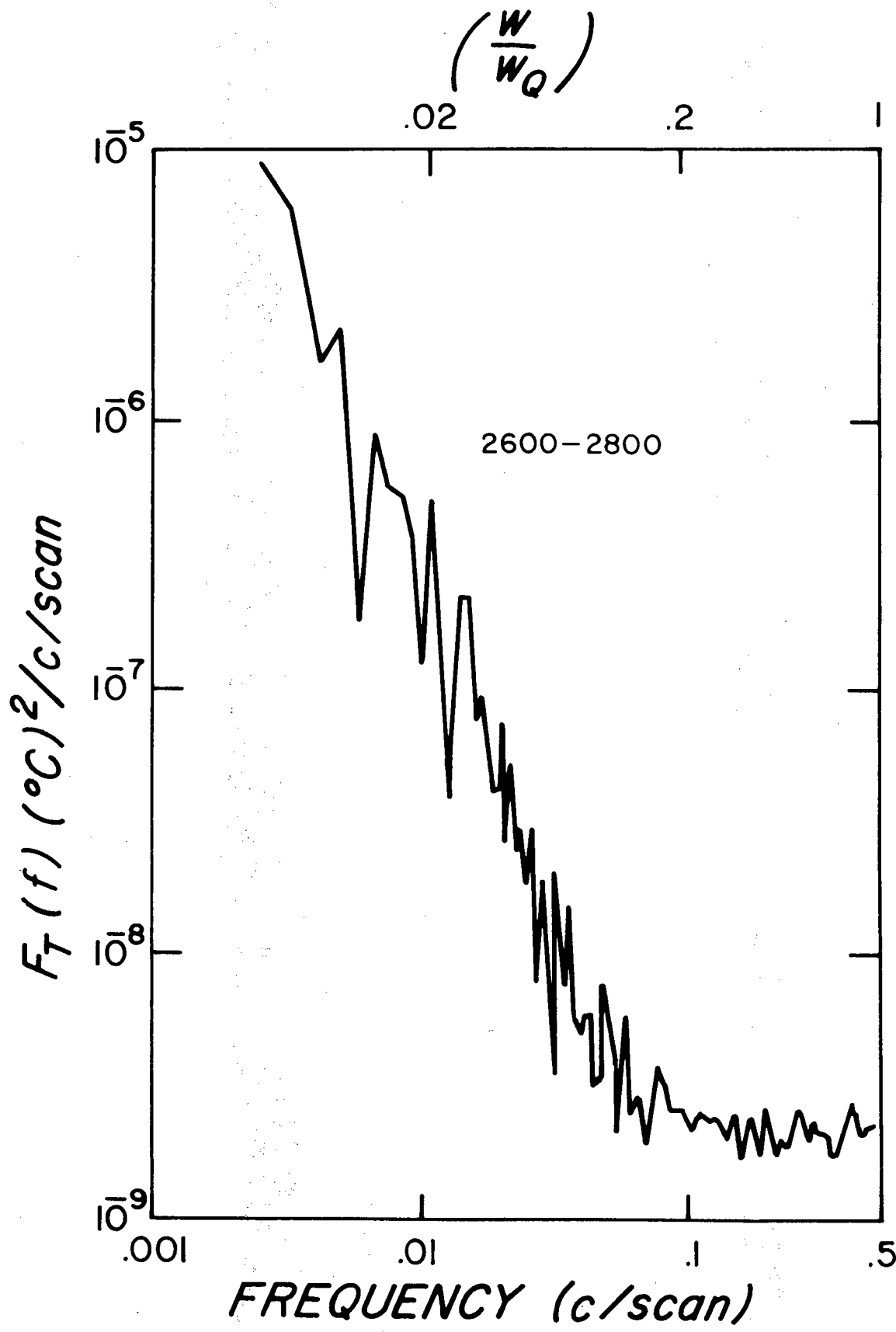


Figure 10b.

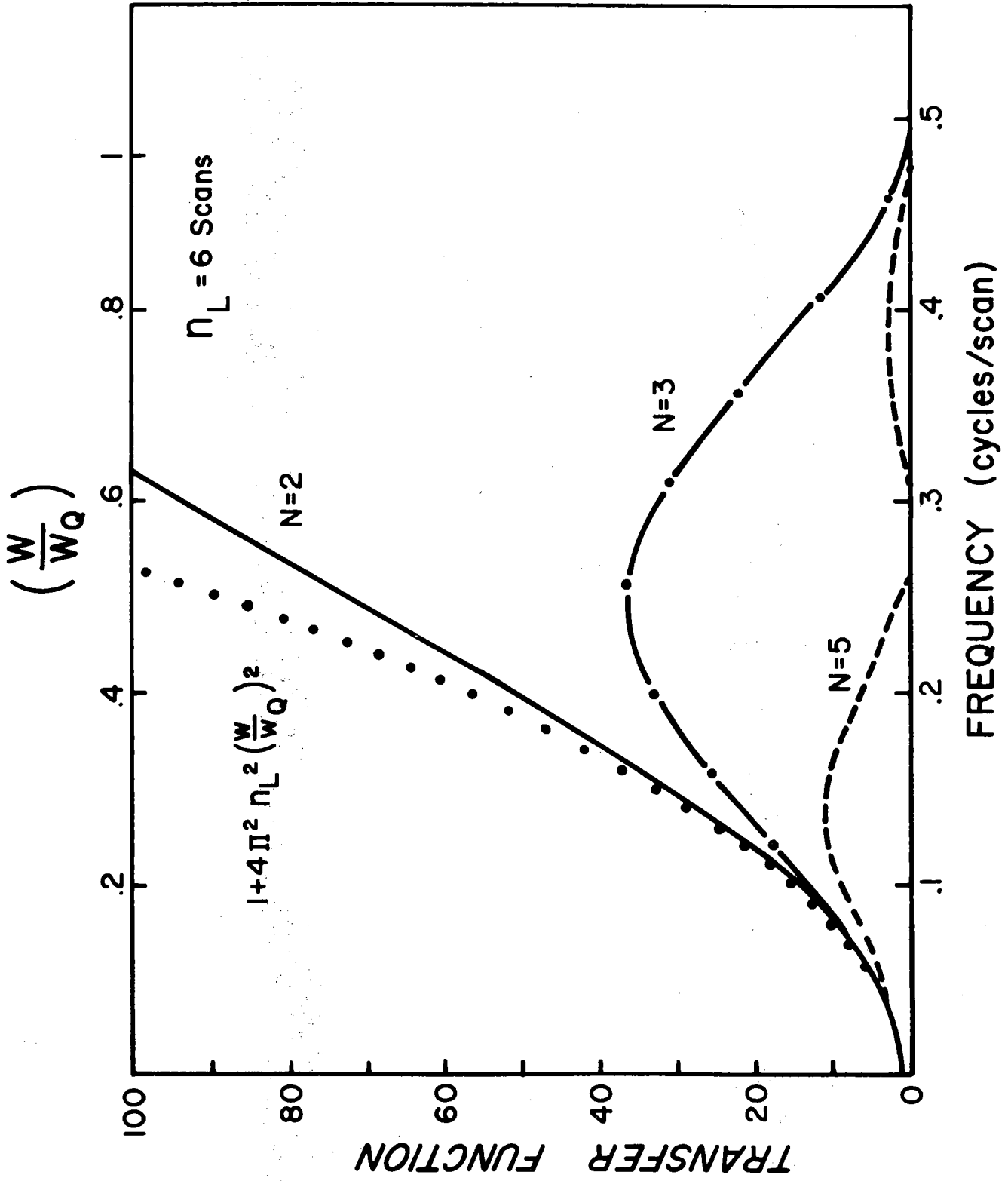


Figure 11.

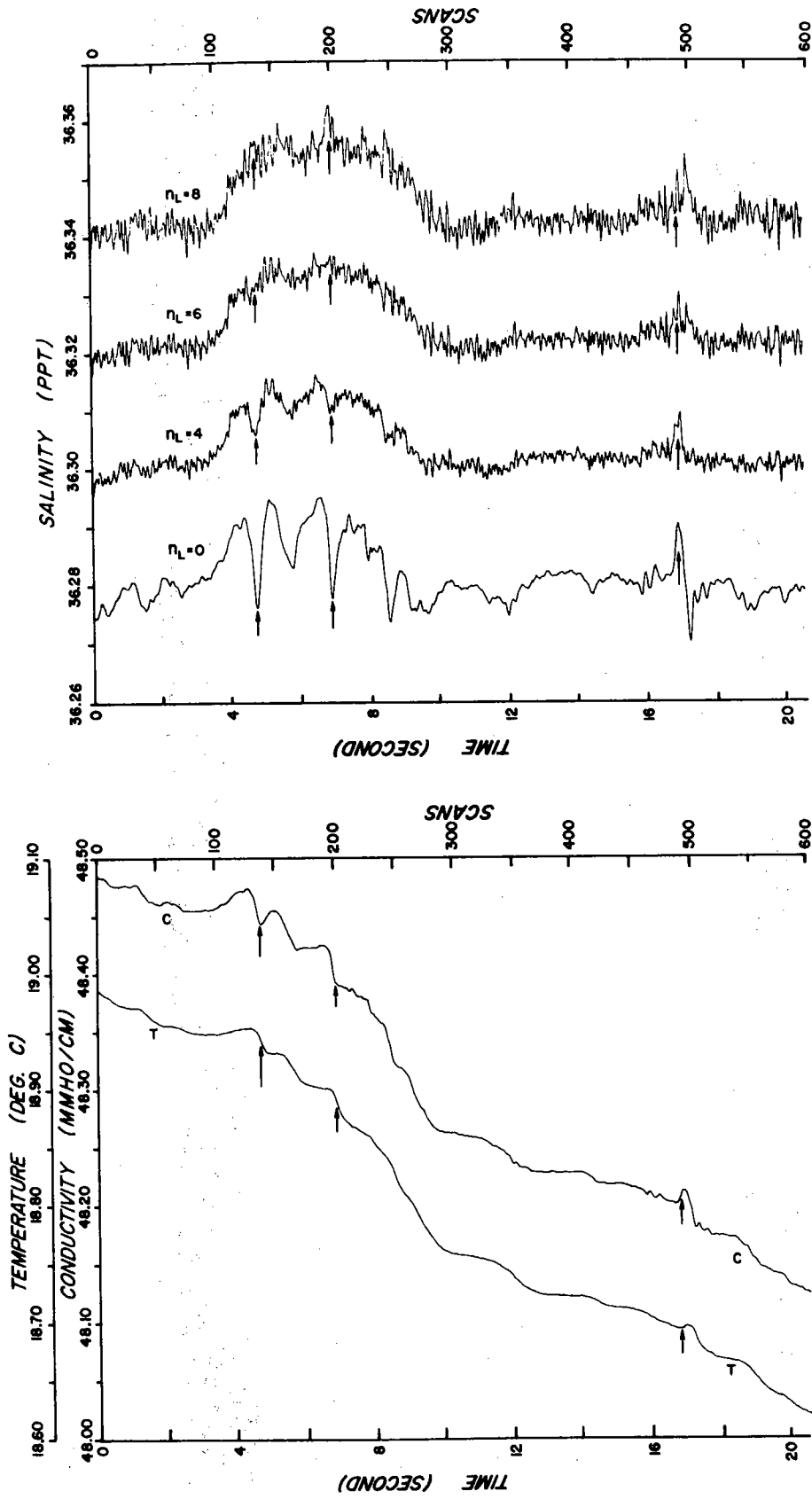


Figure 12.

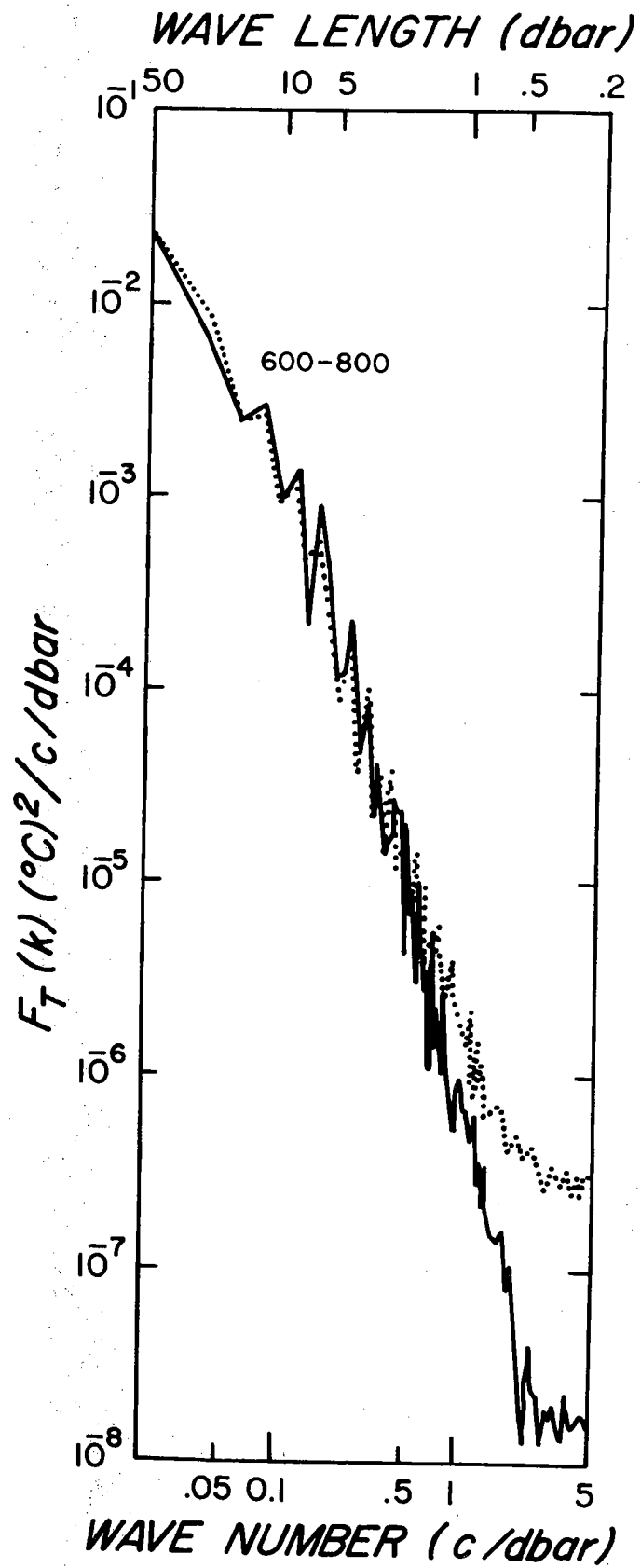


Figure 13.

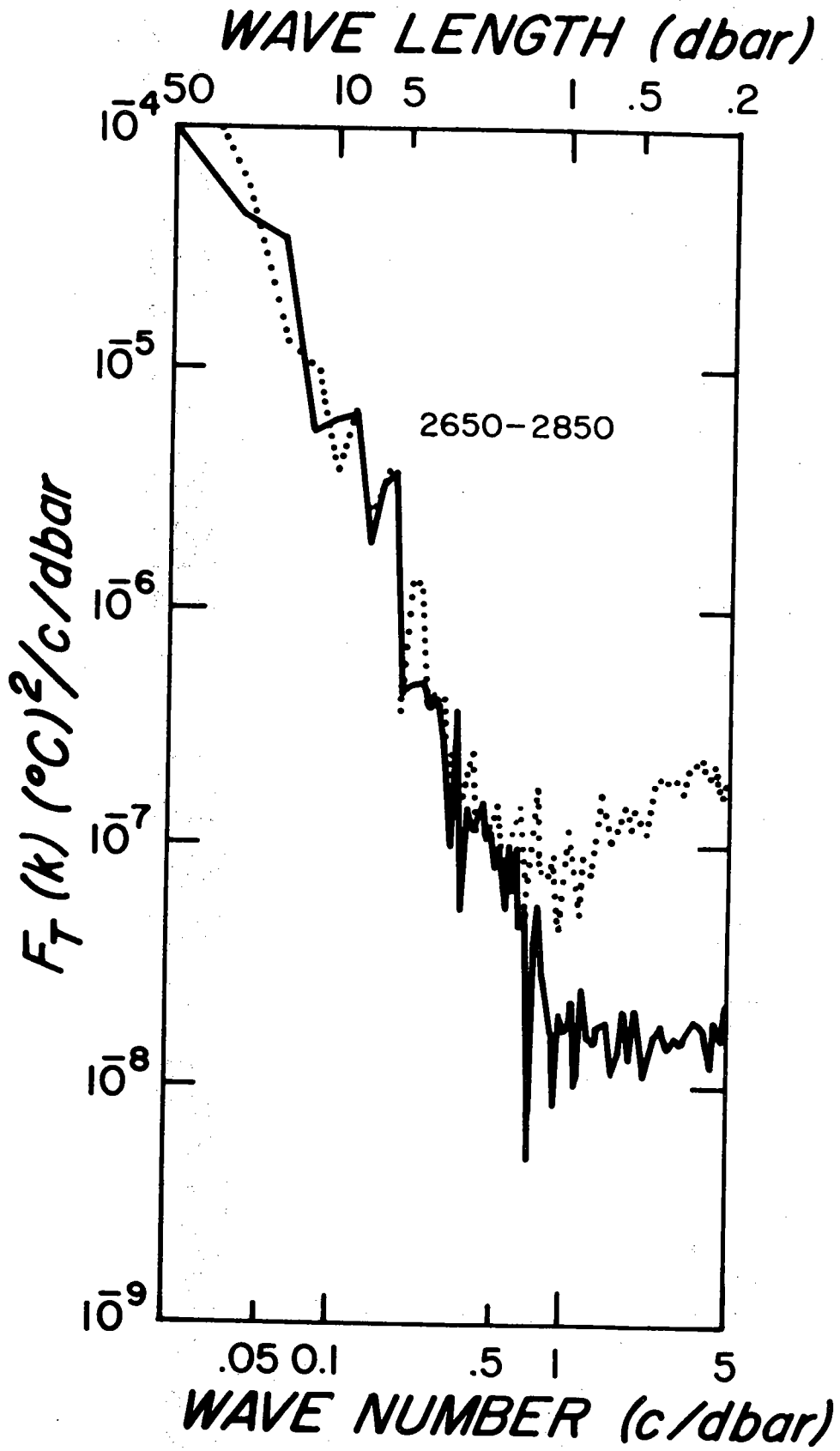


Figure 14.

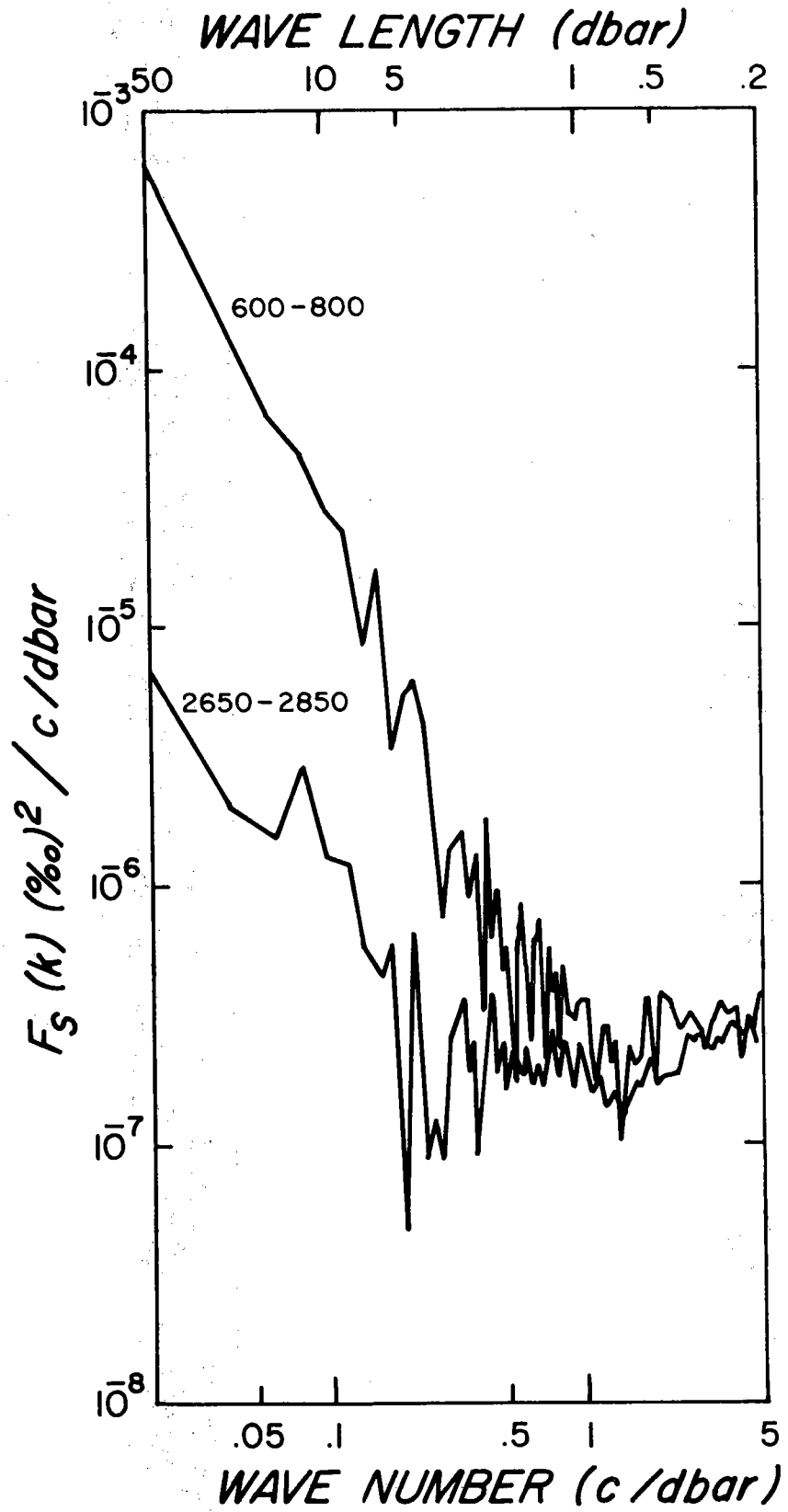


Figure 15.

MANDATORY DISTRIBUTION LIST
 FOR UNCLASSIFIED TECHNICAL REPORTS, REPRINTS, & FINAL REPORTS
 PUBLISHED BY OCEANOGRAPHIC CONTRACTORS
 OF THE OCEAN SCIENCE & TECHNOLOGY DIVISION
 OF THE OFFICE OF NAVAL RESEARCH
 (REVISED FEBRUARY, 1974)

1	Director of Defense Research and Engineering Office of the Secretary of Defense Washington, D. C. 20301 ATTN: Office, Assistant Director (Research)	1	Commander Naval Oceanographic Office Washington, D. C. 20390 ATTN: Code 1640 (Library) ATTN: Code 70
12	Defense Documentation Center Cameron Station Alexandria, Virginia 22314 Office of Naval Research Department of the Navy Arlington, Virginia 22217	1	National Oceanographic Data Center National Oceanic & Atmospheric Administration U.S. Department of Commerce Rockville, Maryland 20852
3	ATTN: Ocean Science & Technology Division, Code 480		
1	ATTN: Naval Applications & Analysis Division, Code 460		
1	ATTN: Code 102-OS		
1	Office of Naval Research Branch Office 495 Summer Street Boston, Massachusetts 02210		
1	LCDR David Cacchione, (USN) ONR Representative Woods Hole Oceanographic Institution Woods Hole, Massachusetts 02543 Director Naval Research Laboratory Washington, D. C. 20390		
6	ATTN: Library, Code 2029 (ONRL)		
6	ATTN: Library, Code 2620		

Woods Hole Oceanographic Institution
WHOI-74-89

W.H.O.I./BROWN CTD MICROPROFILER: METHODS OF CALIBRATION AND DATA HANDLING by N. P. Fofonoff, S. P. Hayes, and R. C. Millard, Jr. 66 pages, December 1974. Contract N00014-74-C0262; NR 083-004.

This report describes calibration techniques developed over the past three years for the WHOI/Brown CTD in the Moored Array Program. Comparison is made with classical methods of hydrography for stations obtained in the MODE-1 density program. Methods for temperature lag correction and conversion of conductivity to salinity are given.

1. CTD
2. Calibration
3. Salinity

- I. Fofonoff, N. P.
- II. Hayes, S. P.
- III. Millard, R. C., Jr.
- IV. N00014-74-C0262; NR 083-004

This card is UNCLASSIFIED

Woods Hole Oceanographic Institution
WHOI-74-89

W.H.O.I./BROWN CTD MICROPROFILER: METHODS OF CALIBRATION AND DATA HANDLING by N. P. Fofonoff, S. P. Hayes, and R. C. Millard, Jr. 66 pages, December 1974. Contract N00014-74-C0262; NR 083-004.

This report describes calibration techniques developed over the past three years for the WHOI/Brown CTD in the Moored Array Program. Comparison is made with classical methods of hydrography for stations obtained in the MODE-1 density program. Methods for temperature lag correction and conversion of conductivity to salinity are given.

1. CTD
2. Calibration
3. Salinity

- I. Fofonoff, N. P.
- II. Hayes, S. P.
- III. Millard, R. C., Jr.
- IV. N00014-74-C0262; NR 083-004

This card is UNCLASSIFIED

Woods Hole Oceanographic Institution
WHOI-74-89

W.H.O.I./BROWN CTD MICROPROFILER: METHODS OF CALIBRATION AND DATA HANDLING by N. P. Fofonoff, S. P. Hayes, and R. C. Millard, Jr. 66 pages, December 1974. Contract N00014-74-C0262; NR 083-004.

This report describes calibration techniques developed over the past three years for the WHOI/Brown CTD in the Moored Array Program. Comparison is made with classical methods of hydrography for stations obtained in the MODE-1 density program. Methods for temperature lag correction and conversion of conductivity to salinity are given.

1. CTD
2. Calibration
3. Salinity

- I. Fofonoff, N. P.
- II. Hayes, S. P.
- III. Millard, R. C., Jr.
- IV. N00014-74-C0262; NR 083-004

This card is UNCLASSIFIED

Woods Hole Oceanographic Institution
WHOI-74-89

W.H.O.I./BROWN CTD MICROPROFILER: METHODS OF CALIBRATION AND DATA HANDLING by N. P. Fofonoff, S. P. Hayes, and R. C. Millard, Jr. 66 pages, December 1974. Contract N00014-74-C0262; NR 083-004.

This report describes calibration techniques developed over the past three years for the WHOI/Brown CTD in the Moored Array Program. Comparison is made with classical methods of hydrography for stations obtained in the MODE-1 density program. Methods for temperature lag correction and conversion of conductivity to salinity are given.

1. CTD
2. Calibration
3. Salinity

- I. Fofonoff, N. P.
- II. Hayes, S. P.
- III. Millard, R. C., Jr.
- IV. N00014-74-C0262; NR 083-004

This card is UNCLASSIFIED

SECURITY CLASSIFICATION OF THIS PAGE (When Data Entered)

REPORT DOCUMENTATION PAGE		READ INSTRUCTIONS BEFORE COMPLETING FORM
1. REPORT NUMBER WHOI-74-89	2. GOVT ACCESSION NO.	3. RECIPIENT'S CATALOG NUMBER
4. TITLE (and Subtitle) W.H.O.I./BROWN CTD MICROPROFILER: METHODS OF CALIBRATION AND DATA HANDLING		5. TYPE OF REPORT & PERIOD COVERED Technical
		6. PERFORMING ORG. REPORT NUMBER
7. AUTHOR(s) N. P. Fofonoff, S. P. Hayes, and R. C. Millard, Jr.		8. CONTRACT OR GRANT NUMBER(s) N00014-74-C0262;
9. PERFORMING ORGANIZATION NAME AND ADDRESS Woods Hole Oceanographic Institution Woods Hole, MA 02543		10. PROGRAM ELEMENT, PROJECT, TASK AREA & WORK UNIT NUMBERS NR 083-004
11. CONTROLLING OFFICE NAME AND ADDRESS Office of Naval Research Code 480		12. REPORT DATE December 1974
		13. NUMBER OF PAGES 66
14. MONITORING AGENCY NAME & ADDRESS (if different from Controlling Office)		15. SECURITY CLASS. (of this report) Unclassified
		15a. DECLASSIFICATION/DOWNGRADING SCHEDULE
16. DISTRIBUTION STATEMENT (of this Report) Approved for public release; distribution unlimited.		
17. DISTRIBUTION STATEMENT (of the abstract entered in Block 20, if different from Report)		
18. SUPPLEMENTARY NOTES		
19. KEY WORDS (Continue on reverse side if necessary and identify by block number) 1. CTD 2. Calibration 3. Salinity		
20. ABSTRACT (Continue on reverse side if necessary and identify by block number) This report describes calibration techniques developed over the past three years for the WHOI/Brown CTD in the Moored Array Program. Comparison is made with classical methods of hydrography for stations obtained in the MODE-1 density program. Methods for temperature lag correction and conversion of conductivity to salinity are given.		